AD648411

AD

TR-1330

AN ARTILLERY SIMULATOR FOR FUZE EVALUATION

by

Herbert D. Curchack

November 1966

ARCHIVE COPY

DDC
MAR 17 1967
D

U.S. ARMY MATERIEL COMMAND

HARRY DIAMOND LABORATORIES

WASHINGTON, D.C. 20438

DISTRIBUTION OF THIS DOCUMENT IS UNLIMITED

The findings in this report are not to be construed as an official Department of the Army position, unless so designated by other authorized documents.

Destroy this report when it is no longer needed. Do not return it to the originator.

AD

DA-1P523801A301
AMCMS Code: 5522.11.62500
HDL Proj 36500

TR-1330

AN ARTILLERY SIMULATOR FOR FUZE EVALUATION

by

Herbert D. Curchack

November 1966

U.S. ARMY MATERIEL COMMAND
HARRY DIAMOND LABORATORIES
WASHINGTON, D.C. 20438

DISTRIBUTION OF THIS DOCUMENT IS UNLIMITED

CONTENTS

ABSTRACT 5

1. INTRODUCTION 5

2. THE CONCEPT. 6
   2.1 The Gas Gun 7
   2.2 The Rotatable Tube 9
   2.3 The Method of Stopping. 11
   2.4 The Readout System. 15

3. CONSTRUCTION AND INSTRUMENTATION 18

4. PERFORMANCE. 21
   4.1 Gas Gun 21
   4.2 Spin Catcher 30
   4.3 Stopping Mechanism. 30
      4.3.1 Linear Deceleration. 34
      4.3.2 Angular Acceleration 37
      4.3.3 Improvements in Stopping Mechanism . . 39
   4.4 Readout 39

5. CONCLUSION AND RECOMMENDATIONS 41

6. REFERENCES 42

Appendix A.—Trajectory of Bird from Muzzle to Spin Catcher 45
Appendix B.—Gas Gun Performance 47
Appendix C.—Computation of Average Deceleration of the Bird 51
Appendix D.—Expression of Efficiency in Terms of Lengths and Accelerations. 58

BLANK PAGE

ABSTRACT

A simulator has been constructed at the Harry Diamond Laboratories for testing fuzes in an environment that provides linear and angular accelerations simultaneously as they are applied in rifled artillery weaponry. Electrical interrogation of the fuze is made during this time and subsequently while the angular velocity is maintained.

This report contains a description of the device and a discussion of certain specific aspects of performance. It is meant to be an introduction to the technique employed, and a guide for future research and development. The performance, some results obtained, and the manner in which the simulation may be improved are described.

1. INTRODUCTION

Centrifuges, spinners, air or gas guns, actuators and rocket sleds have been constructed for laboratory simulation of the forces experienced by fuzes or fuze components when launched or fired. Of these, gas guns and spinners are most frequently used by engineers concerned with the environment experienced by spinning artillery fuzes such as may be fired from howitzers, recoilless rifles or certain mortars.

In one gas gun technique, the fuze is slowly accelerated to a predetermined velocity and then is violently decelerated upon impact with a known target. This rapid deceleration simulates the setback of the field fired projectile. The main advantages of this technique are that the fuze is immediately available for inspection and the cost and problems associated with recovery in the field are eliminated.

In spinners the fuzes are rotated at the angular velocity appropriate to the weapon and observations are made of performance. These observations may be made by optical or electrical techniques while the fuze is spinning. In addition, some spinners use low inertia motors or other means in an effort to duplicate the angular accelerations experienced in the field.

This report describes a facility constructed at the Harry Diamond Laboratories that unites the features of the gas gun and the low inertia spinner so that setback occurs simultaneously with spin acceleration. It contains an examination of the device in general, occasionally delving into the specifics of some aspects of performance. It is an introduction to the

technique employed, and a guide for future research and development. The performance, some results obtained, and the manner in which the simulation may be improved are described.

2. THE CONCEPT

A system is desired in which the applied linear and angular accelerations on a fuze or fuze component are simultaneous as in projectiles fired from rifled barrels. The angular velocity achieved is to be maintained and fuzing components electrically monitored during times representative of the flight times of the actual projectile. Our approach is as follows:

Consider a hollow cylindrical tube rotating about its longitudinal axis at a desired angular velocity. Allow a projectile (which we shall call "bird" to distinguish it from the actual projectile used in the field) to enter the tube at a given linear velocity. Within the tube the bird is to decelerate in its linear motion while accelerating in its angular motion until it has stopped its linear movement and acquired the angular velocity of the spinning tube. Furthermore, at some time during this process an electrical circuit is to be completed that allows continuous monitoring of the fuzing component within the bird.

The problems associated with this approach are readily enumerated and must be properly resolved. It is necessary to:

(1) Provide the requisite linear velocity to the bird without disturbing the fuze component. (Sections 2.1, 4.1)

(2) Construct a tube (spin-catcher), of bore sufficient for testing fuze components, that can rotate at a representative angular velocity. (Sections 2.2, 4.2)

(3) Provide a stopping mechanism to decelerate the bird properly while minimizing the forces transmitted to the bearings (section 2.3, 4.3).

(4) Provide electrical circuits from the bird to the spinning tube to remote instrumentation. (Sections 2.4, 4.4)

These problems are interdependent; for example, (2) must embody (4). However, the unique features of each item were analyzed and developed separately resulting in useful numerical representations.

For ideal simulation of field conditions, the bird containing the fuze component should be stopped in a distance equivalent to the length of the field artillery piece from which the component is fired. If the artillery barrel is 10 ft, s should be approximately 10 ft and from previous considerations L should be on the order of 1000 ft. The available space limited our prototype gas gun to an L of 30 ft which reduced s to about 6 in. and limits v to $\sqrt{a/2}$ where a is in ft/sec^2 and v is in ft/sec. For a typical a of 20,000 g (640,000 ft/sec^2), v is less than 600 ft/sec, which is easily attainable in gas guns.

The bore of the gun was chosen to be 2 in. because this is large enough to accommodate many fuzing components yet small enough to allow for an easily constructed rotating catch tube.

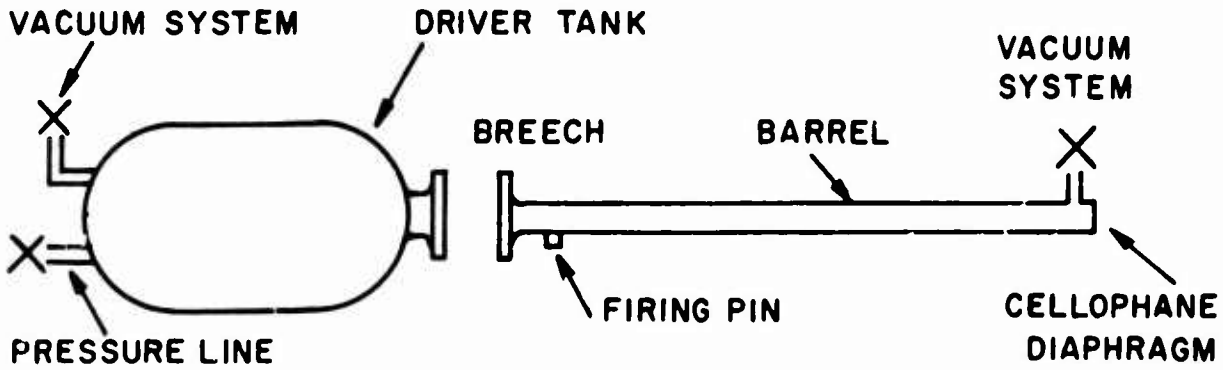

Figure 1. Gun arrangement diagram.

The gun (fig. 1) has a barrel constructed from 1/4-in. wall, 2 1/2-in. OD steel tubing. The driver is a converted 3.2-ft^3 air storage tank. The bird is a right circular cylinder approximately 4 in. long and usually weighs between 1 and 2 lb. The bird is inserted into the breech of the gun up to the firing pin. A cellophane diaphragm a few-thousandths of an inch thick is placed over the muzzle of the gun and the barrel is evacuated to 10 to 100 μ Hg. The bird, diaphragm, and firing pin are sealed with O-rings. The gun can then be fired in either of two ways. The pin may be pulled without attaching the driver to the gun. In this case the 14.7-psi atmospheric pressure propels the bird. Furthermore, there is effectively no pressure difference across the bird as it leaves the gun. (This will later be shown to be a distinct advantage.)

The second method involves attaching the driver to the barrel, evacuating this tank through an auxiliary vacuum system, pressurizing it with the proper amount of helium gas, and then pulling the firing pin. Helium gas is used because (1) its light molecular weight makes it a more efficient gas than air in maintaining a constant acceleration in the gun; (2) it is safer than the most efficient gas, hydrogen; (3) it disperses more efficiently than air after the bird leaves the muzzle. (This

2.1 The Gas Gun

The method of setback simulation most often used at HDL is to first accelerate a bird in a 96-ft air gun and then stop it within a few inches in a target of lead blocks (ref 1). The velocity attained in the gun is chosen so that the peak deceleration on impact as recorded by a copper ball accelerometer (ref 2,3,4) is comparable with typical field conditions. Therefore, the simulation is based only on the magnitude of the peak force not its duration. Nevertheless, this air gun facility has proved its usefulness in the development of many electromechanical fuzing systems because the fuze designer has had a test readily available that his fuze had to survive before it could work properly in the field.

If we assume an average acceleration $\bar{a}$ that is one-half the peak acceleration a, the velocity at impact v to produce a given a in the stopping distance s is approximately

$$v \approx \sqrt{2\bar{a}\ s} \tag{1}$$

or

$$v \approx \sqrt{a\ s} \tag{2}$$

Equation (2), as verified by a good deal of experimental evidence, is adequate to within about 20 percent (which is the precision of both a and s).

The velocity we need to attain in our gas gun is immediately available in terms of simulation parameters a and s. Assume that the velocities of interest can be obtained in an almost constant acceleration gun, therefore

$$v = \sqrt{2\ a_g L} \tag{3}$$

where a_g is the acceleration and L is the length of the gas gun. From (1) and (3)

$$a_g/\bar{a} = s/L \tag{4}$$

Since, as previously stated, the gun force or acceleration is to be small compared with the stopping force

$$s/L \ll 1 \tag{5}$$

will also be shown to be a very distinct advantage.) Although there has been no need and therefore no effort to obtain velocities higher than 600 ft/sec, a velocity of 2500 ft/sec with a 1-lb bird is a conservative upper limit for the gun.

2.2 The Rotatable Tube

For proper simulation the rotating tube (spin-catcher) must rotate the bird about its longitudinal axis, and therefore the bird must be a reasonably close fit to the bore of the tube. For this reason a 3-ft section of the same steel tubing used for the gun barrel was chosen for the first tube. The outside of the tube was then machined to be concentric with the inside, a ball bearing was mounted at each end, and a sheave was provided for a single v-belt (fig. 2).

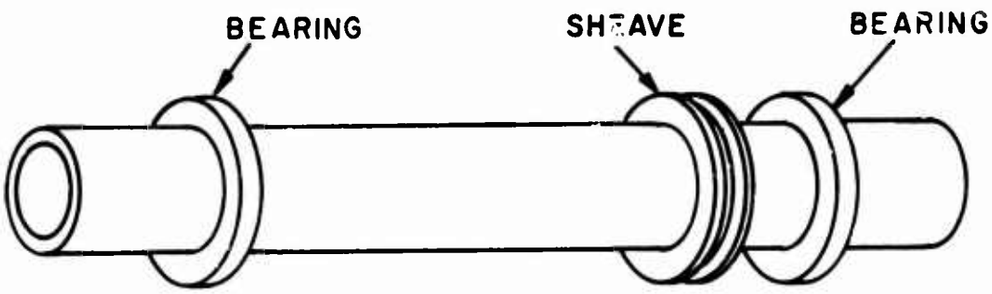

Figure 2. Spinner arrangement diagram.

This assembly was then mounted (by the bearings) on a heavy steel platform and a variable speed motor was provided to impart a drive for the tube. The complete spin-catcher was then installed about 14 in. from the muzzle of the gas gun. Aligning was accomplished with a specially machined tube that fit closely within the gun and spin-catcher.

The two major considerations for the location of the spin-catcher were that the device be close enough to the muzzle so that the bird would enter without hitting the tube wall, yet far enough so that the driver gas is adequately vented and does not continue to push the bird within the spin-catch tube. A set of curves showing the drop distance due to gravity as a function of horizontal free travel distance and horizontal velocity (fig. 3) revealed that for an arbitrary minimum velocity of 200 ft/sec, there would be a drop of 0.005 in. in a distance of 1 ft. (Appendix A shows that drag may be neglected, and how these curves were obtained.) The first few shots with this

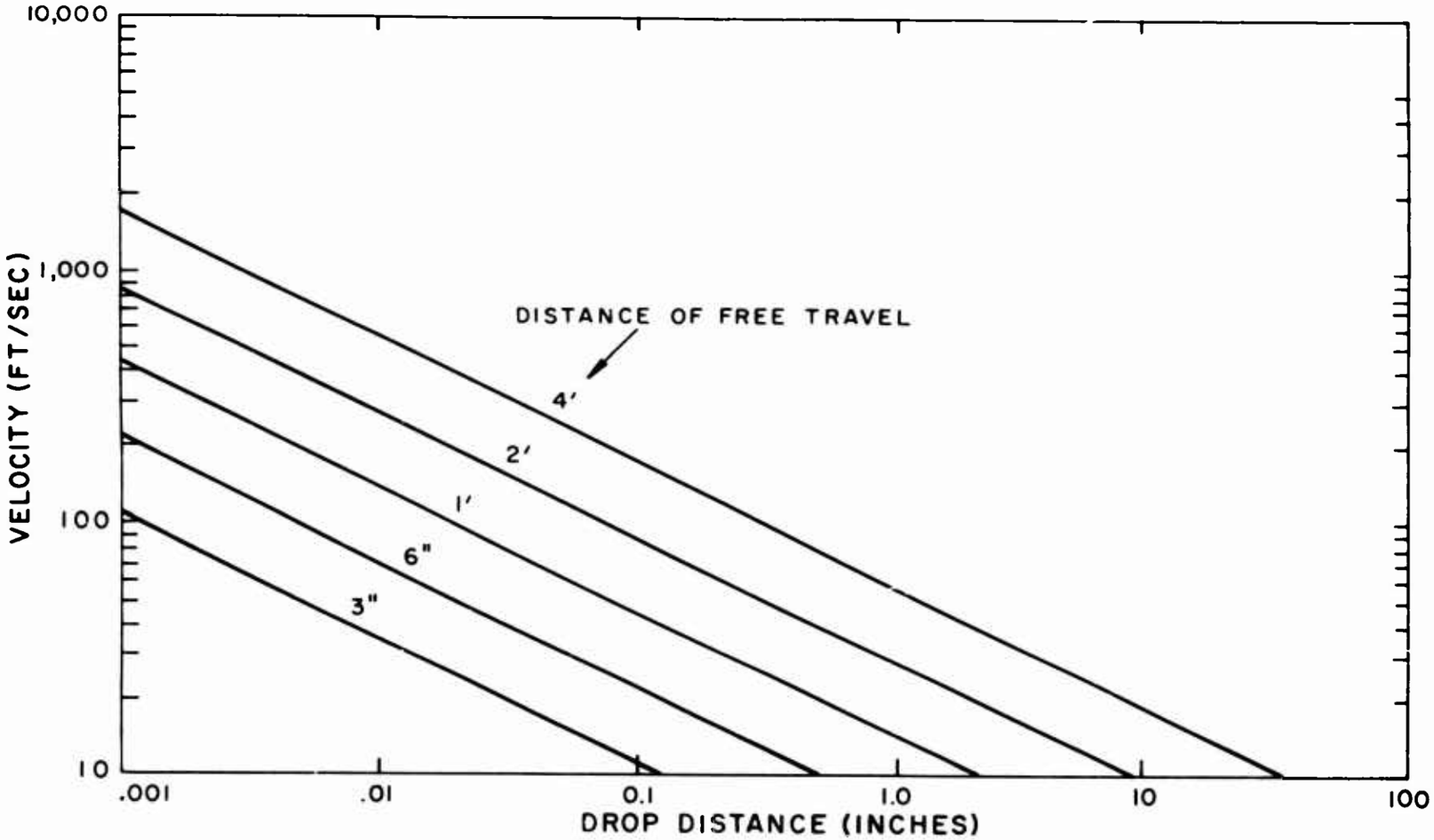

Figure 3. Drop distance versus velocity.

arrangement, however, revealed that the aluminum bird was hitting the spin-catcher wall by as much as 0.030 in. This was eventually traced to a kink in the gun barrel about 30 in. from the muzzle causing the bird to tumble. This was subsequently corrected by reversing the gas gun barrel. No further difficulties with alignment occurred with this spin catcher.

The rotational speed of the spin-catcher at present is limited by the motor to 90 rps (5400 rpm). This is about a factor of 3 less than that desired eventually. A 25-HP d-c motor with the necessary capability has been obtained, but it is expected that there may be belt and bearing difficulties at the higher speeds; these are presently under investigation.

2.3 The Method of Stopping

The conventional HDL air gun technique of stopping the projectile uses lead blocks stacked in a massive steel chamber rigidly attached to a concrete floor. This brute force method is of doubtful use in the spin-catcher for if the catch tube is filled with lead and sealed so that the lead can not come out the far end, the entire momentum impulse will have to be borne by the bearings. At the anticipated high spin rates, we will be at the fringes of bearing technology in this device and such thrust forces would be intolerable. Rather than build thrust bearings into the device (which might be of doubtful utility for high impulses and would undoubtedly decrease the upper rotational limit of the tube) it was decided to use a momentum transfer system.

If an elastic impact occurs between two identical masses in which initially one mass is moving and the other is at rest, the result is that the moving mass stops while the other mass leaves with the initial velocity. (Such an impact is often demonstrated on the billiard table.) There is no expectation that at gas gun velocities we will have, or even want, elastic impacts, but by the proper choice of masses and degrees of inelasticity the bird can always be brought to rest within the spin-catcher while transferring its momentum to a mass which is ejected and eventually stopped by lead blocks.

To catch the bird in these inelastic impacts it is necessary to devise an effective way to absorb the energy not carried off by the momentum exchange mass, or "mem." If the bird is allowed to impact a steel mem, the excess energy will be absorbed in crushing and distortion of the bird, which is highly undesirable. Currently, we use a column of plywood blocks as an intermediary between the bird and the mem with

Fig. 4 Bird, Mem, and Plywood Stack as Used in Artillery Simulator.

1117-65

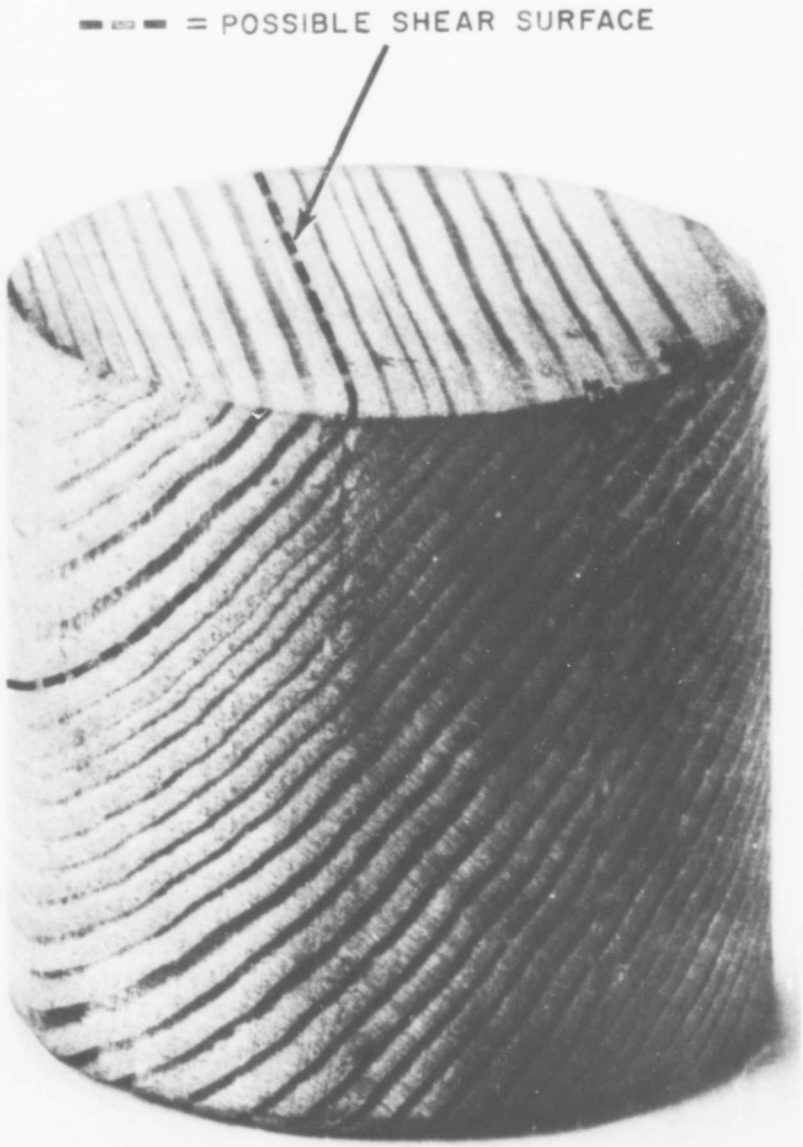

1226-66

Fig. 5 Energy Absorbing Block Cut From a White Pine Two-by-Four.

very effective results. About 150 birds have been caught successfully with only one exception.

After the bird is caught it is held by friction only within the spin-catcher. Therefore, if the driver gas does not readily expand and dissipate between the muzzle and the spin-catcher, it will blow the bird right out of the tube. This was experimentally verified in one shot in which high pressure air was used as the driver gas and is the exception cited above. This explains the desirability of keeping as low a pressure as possible within the gun. If the range of velocities is to extend upward so that gas at higher pressures is used, the spin-catcher will undoubtedly have to be moved further from the muzzle.

Preliminary tests revealed that the length of a column of wood necessary for proper stopping distance (6 in.) is about 2 ft. Currently this column is made up of triangular or square blocks of 3/4-in. plywood (fig. 4). Plywood is used since it assures that the wood compresses in the direction perpendicular to the grain. Some early tests with blocks cut from pine two-by-fours failed in the following way. The crushing of the wood between the bird and the mem caused the blocks to shear along grain surfaces and slip (fig. 5). This wedged the wood so effectively within the tube, that the only way of removing the wood was to drill it out. A similar difficulty was encountered when circular rather than triangular or square disks were used. In this case, the small change in dimension that occurs in the direction normal to the spinner axis is sufficient to pack the wood tightly in the tube. An additional difficulty is seen when the stack of wood is examined as a column (fig. 6).

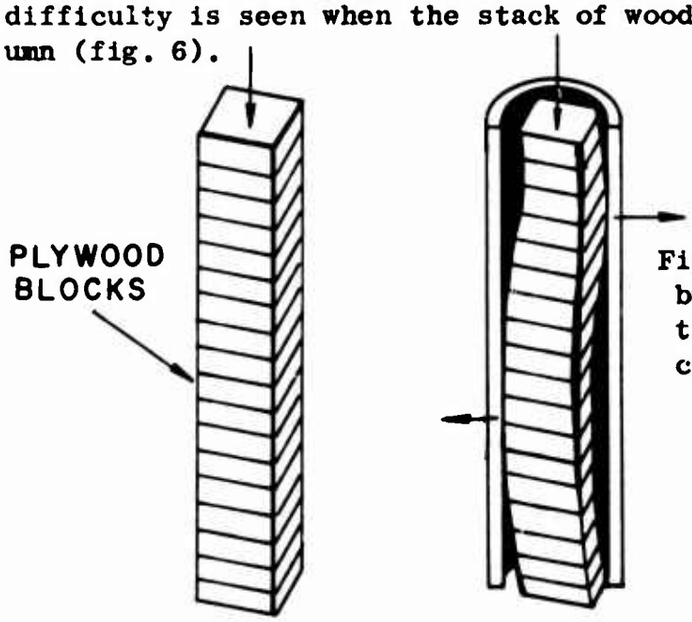

Figure 6. Manner in which buckling results in high transverse forces on the catch tube walls.

The compressive forces make the column buckle. This does not result in severe packing but can introduce considerable transverse forces, which by friction are transmitted through the walls of the tube to the bearings. This buckling is accentuated by knots or voids in the plywood and so only clear wood is being used. For the higher impact velocities the column is supported by a central wooden shaft and aluminum or plastic "spiders" spaced every third or fourth block (fig. 7). The spiders ride on the inner walls of the tube while the wood is slightly undersized. Since the spiders do not change dimension, the packing problem is reduced and the central shaft reduces the buckling problem. A hole is drilled through the mem to allow the shaft a place to travel since it does not compress as readily as the plywood. Special materials such as aluminum honeycomb are available for energy absorbers (ref 5) and will be investigated further.

The question of how quickly the bird achieved the spin of the spin-catcher was initially answered by high-speed motion pictures. A thin rod with a "flat" at one end was attached to the bird. As the bird entered the catcher the end of the rod remained external to the spinner and was photographed. The bird acquired the spinner motion within the time taken for the spinner to make one revolution.

These pictures revealed a rather strange occurrence. The bird entered the spinner and bounced back slightly, which is to be expected for certain cases; then the bird moved slightly forward again. This could not be explained by assuming that the driver gas continued pushing, because these were "vacuum" shots and the pressure behind the bird in the gun was less than atmospheric pressure. It was found that the bird entering the spin-catcher effectively sealed that end of the tube leaving only a small volume of gas around the wood, between the bird and the mem. As the mem travelled down the tube it increased the volume tremendously and the gas pressure dropped severely. Therefore, atmospheric pressure forced the bird forward until the mem left the tube. This effect was eliminated by using a mem of hexagonal cross section.

2.4 The Readout System

To demonstrate the feasibility of the spin-catch method the first 100 shots were made in a catcher with no readout capability. A simple readout system was then designed to complete the system development. This required construction of a second spin-catcher and modification of the bird.

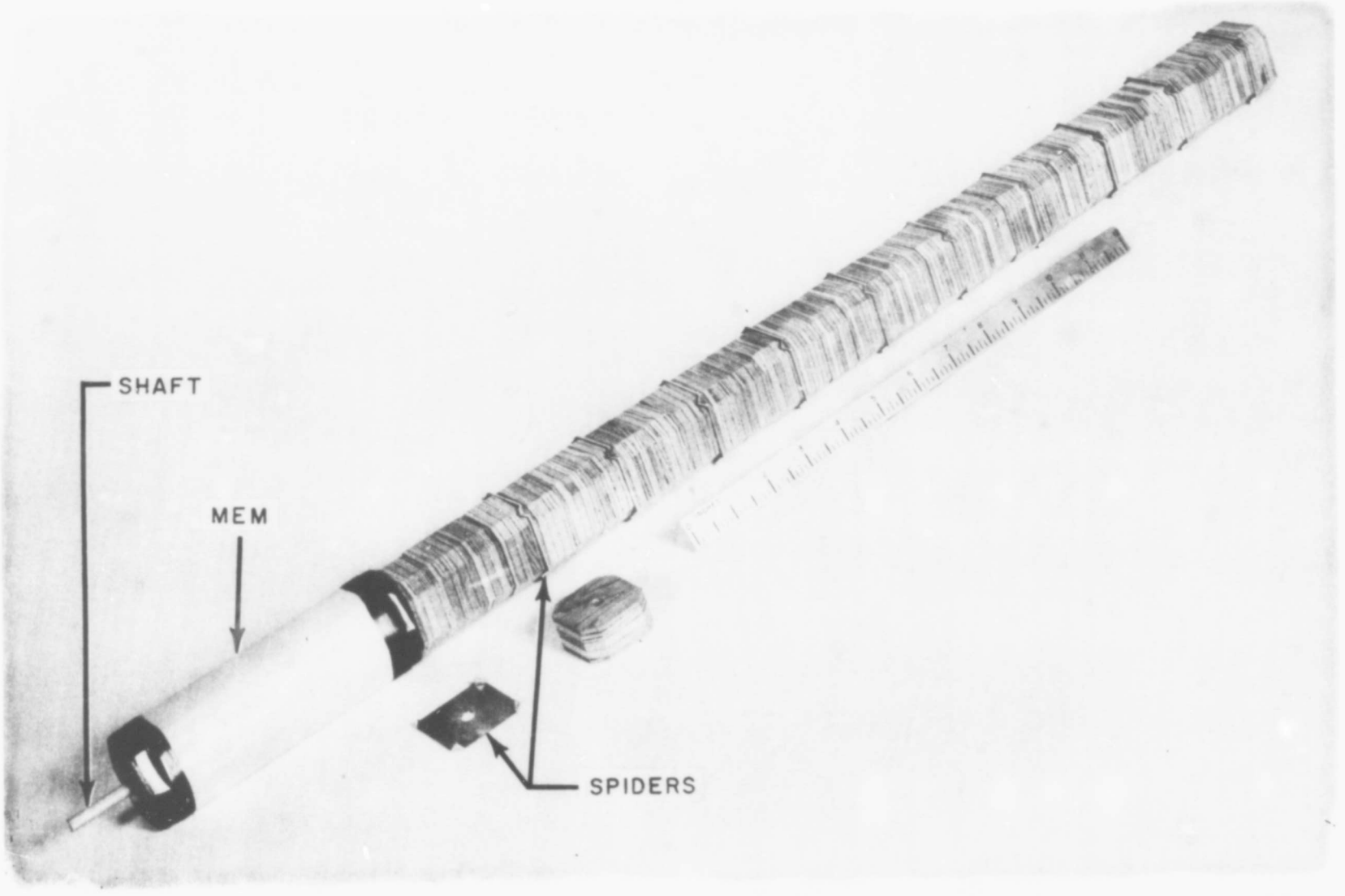

1026-66

Fig. 7 Stopping Assembly Using Shaft and Spiders to Reduce Buckling.

The idea behind the readout is to split the spin-catch tube longitudinally into two or more sections, each insulated electrically from the others and each connected to its own slip ring (fig. 8) and external brush assemblies.

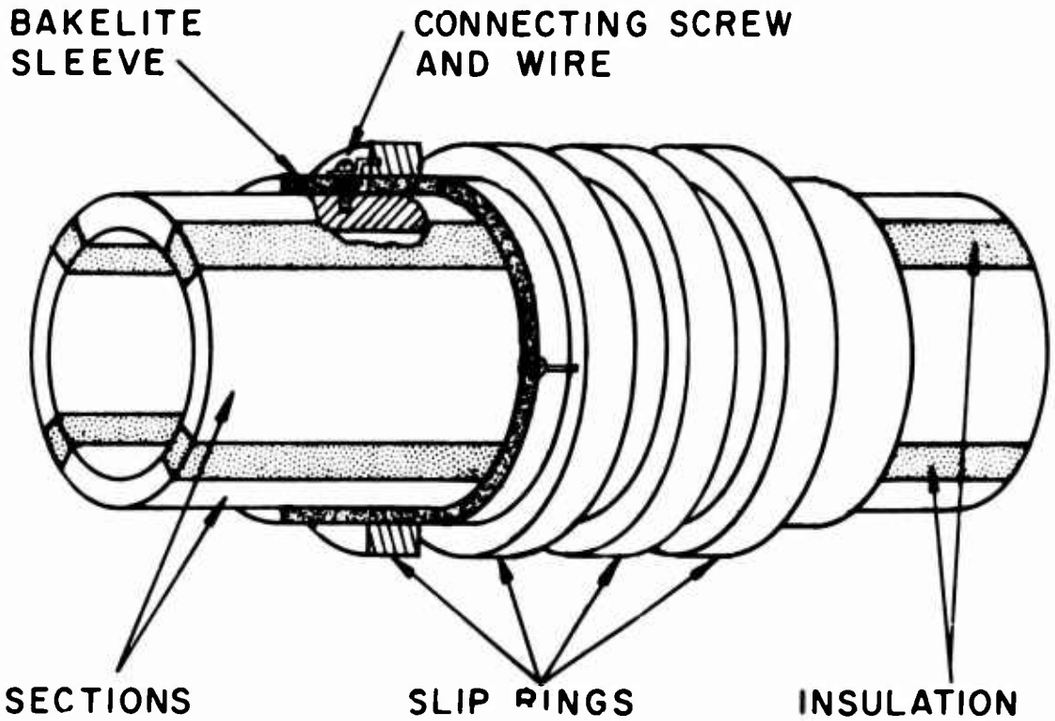

Figure 8. Readout section diagram.

The bird is insulated to preclude its forming any electrical path between sections and carries on it the same number of contacts as there are segments in the catcher. These contacts are allowed limited outward motion and are activated by centrifugal or setback forces (fig. 9).

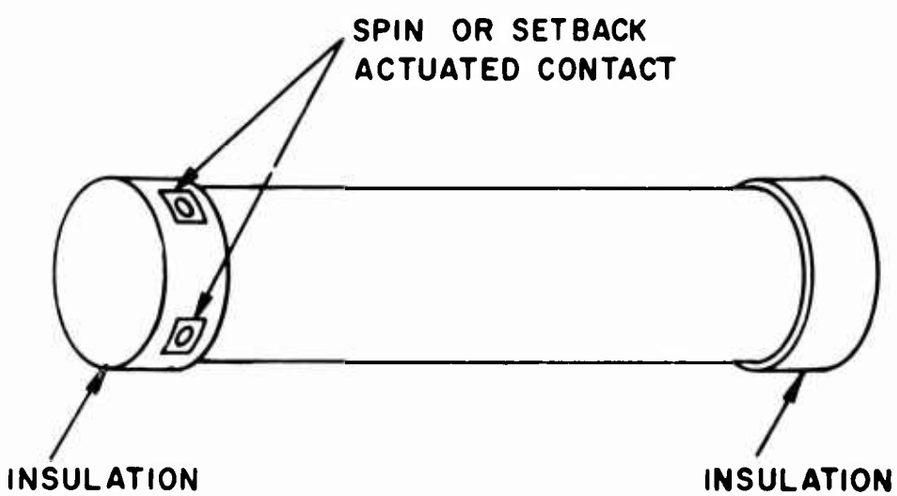

Figure 9. Readout bird diagram.

As soon as the bird enters the spin-catcher and starts rotating or decelerating, the contacts move outward radially, each contacting a single section. If the bird does not achieve the tube's angular velocity immediately, there is relative motion across the sections so that each channel of information is retarded one step for each section traversed. The main advantage of such a design is that it is insensitive to the longitudinal location of the bird, assuring readout as long as the bird is caught.

The spin-catcher with readout that was constructed has two aluminum segments, embedded in epoxy for insulation, and slipped into a steel tube for strength. This resulted in a section about 1 in. larger in outer diameter than the previous spin-catcher. To keep the same size bearings and mounting arrangement the instrumented section was shortened and connected to two bearing sections.

This construction has the disadvantage that the bird must be caught in a somewhat shorter distance; but this has not been a handicap, since for any particular experiment the stopping position has been reproducible to ±3/4 in. In the readout spin-catcher the mem and the stopping material must be electrically insulated from the tube to prevent an electrical short circuit between sections. Precautions must also be taken if there is an O-ring on the bird. Neoprene, which is probably the most common O-ring material, showed a resistance of somewhat less than 10,000 ohms in the configuration used.

3. CONSTRUCTION AND INSTRUMENTATION

The details of the construction of the current system are covered in reference 6. Some idea of the size and arrangement of the apparatus may be gained from figures 10 and 11. In figure 10, the muzzle end of the gas gun protrudes through the wall of a reinforced concrete room, which contains the spin-catcher. The slip ring section of the spin-catcher is visible as is a black box containing two photocells used with the two lamps in the foreground to measure the time of flight of the bird.

The spin-catcher and motor arrangement is shown in figure 11. Also visible is a second black box used to measure the velocity with which the mem leaves the spinner. In the upper right hand corner is a wooden catch box containing lead blocks. This box, which is backed up by a concrete wall is used to catch the mem.

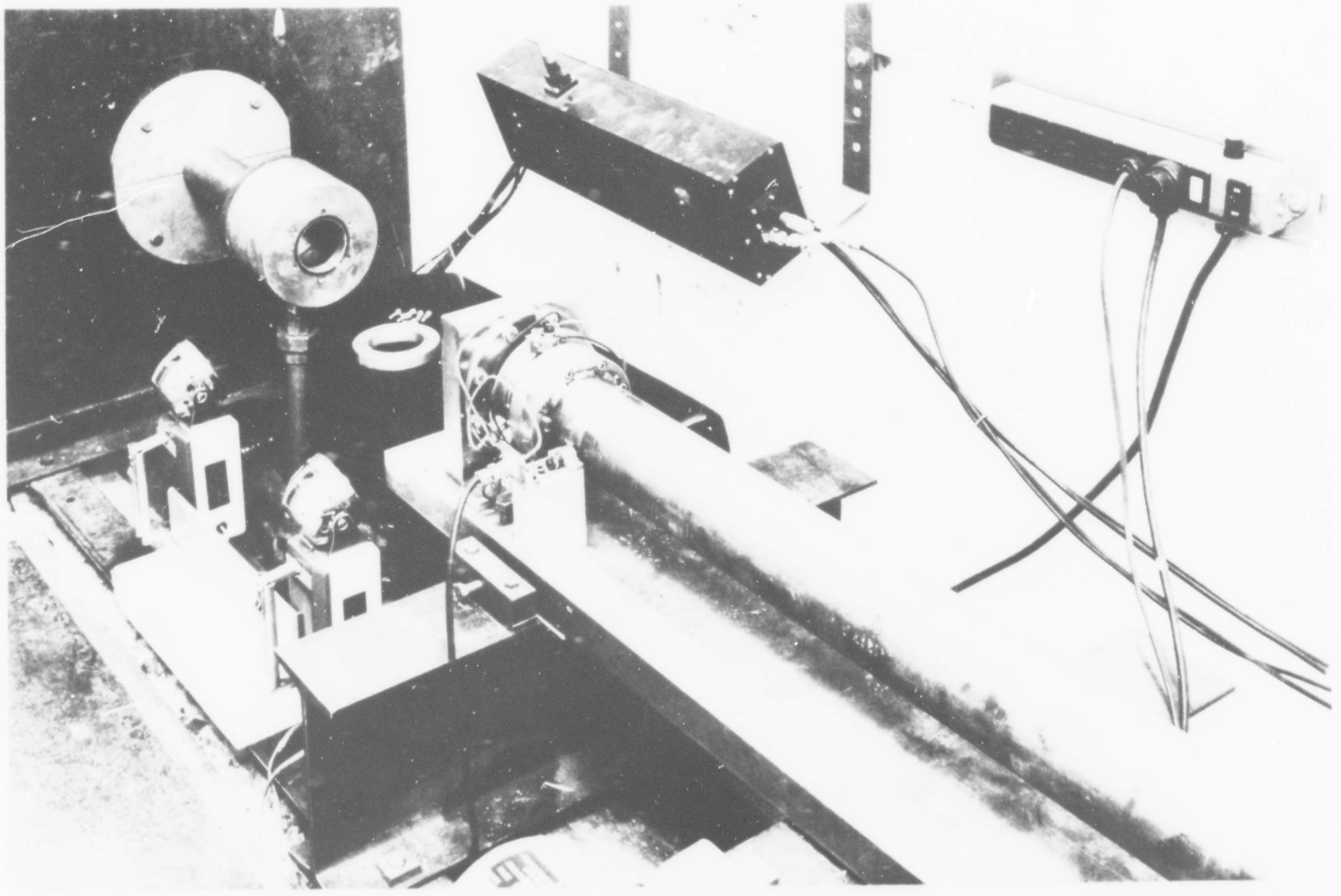

1119-65

Fig. 10 Muzzle End of Gun and Spin-Catcher.

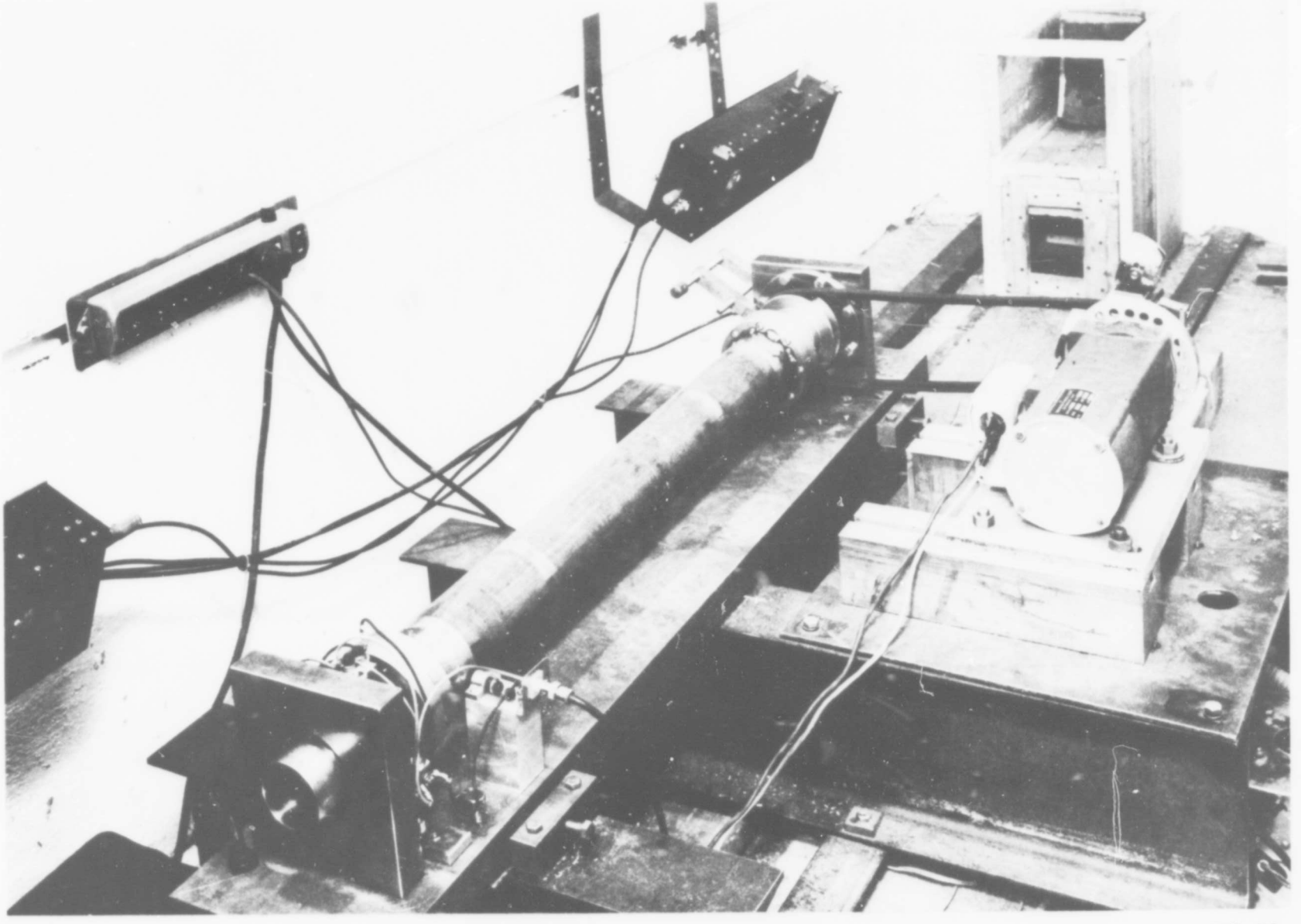

1118-65

Fig. 11 Spin-Catcher and Motor Arrangement.

The remainder of the instrumentation (fig. 12) consists of (1) a vacuum pump to evacuate the gun, (2) pressure gauges, (3) a photocell power supply, (4) two digital timers to measure the time of flight of the bird and mem, (5) a motor speed control autotransformer, (6) a frequency meter to measure the rps of the spin-catcher, (7) an oscilloscope to measure the component output during impact, and (8) a chart recorder to measure the component output from impact until the test is complete. A section of the gun is visible as it enters the concrete catch room. The various other switches are vacuum and firing controls, camera triggers, etc.

4. PERFORMANCE

4.1 Gas Gun

To assign a figure of merit to the performance of the gas gun, it is important to know (for our purposes) what is "perfect" performance, how close we can achieve this performance theoretically, and how well our results agree with the theory.

We shall define a "perfect" gun as one in which the acceleration is constant, since this would be the gun with the lowest peak acceleration for any given length gun and muzzle velocity. Looked at in a slightly different way this is the shortest gun possible for a given peak acceleration and muzzle velocity. In the design of a facility, the length of the gun needed will be an important consideration in cost as well as space. Therefore, if we define the efficiency of the gun (R) to be equal to the ratio of the muzzle velocity to the ideal velocity, then R^2 is the ratio of the length of the ideal gun to the actual length for a particular muzzle velocity (appendix D). Appendix B contains predictions of the velocity achievable in gas guns and bounds for the theoretical efficiency.

The efficiency R as a function of dimensionless velocity $u = v/c$ (where c is the sound speed of the gas used in the gun) is plotted in figure 13 for gases with γ* of 7/5 and 5/3 based upon the model for a constant diameter gun. A constant diameter gun (ref 7) is one in which the gun diameter is maintained both upstream and downstream of the bird for effectively infinite lengths. The theoretical properties of such guns are expressible in closed form and therefore provide insight and a basis for qualitative decisions. Although oversized reservoir guns (ref 8, 9, 10) are somewhat more efficient, their behavior is adequately represented by these curves.

---

*See appendix B

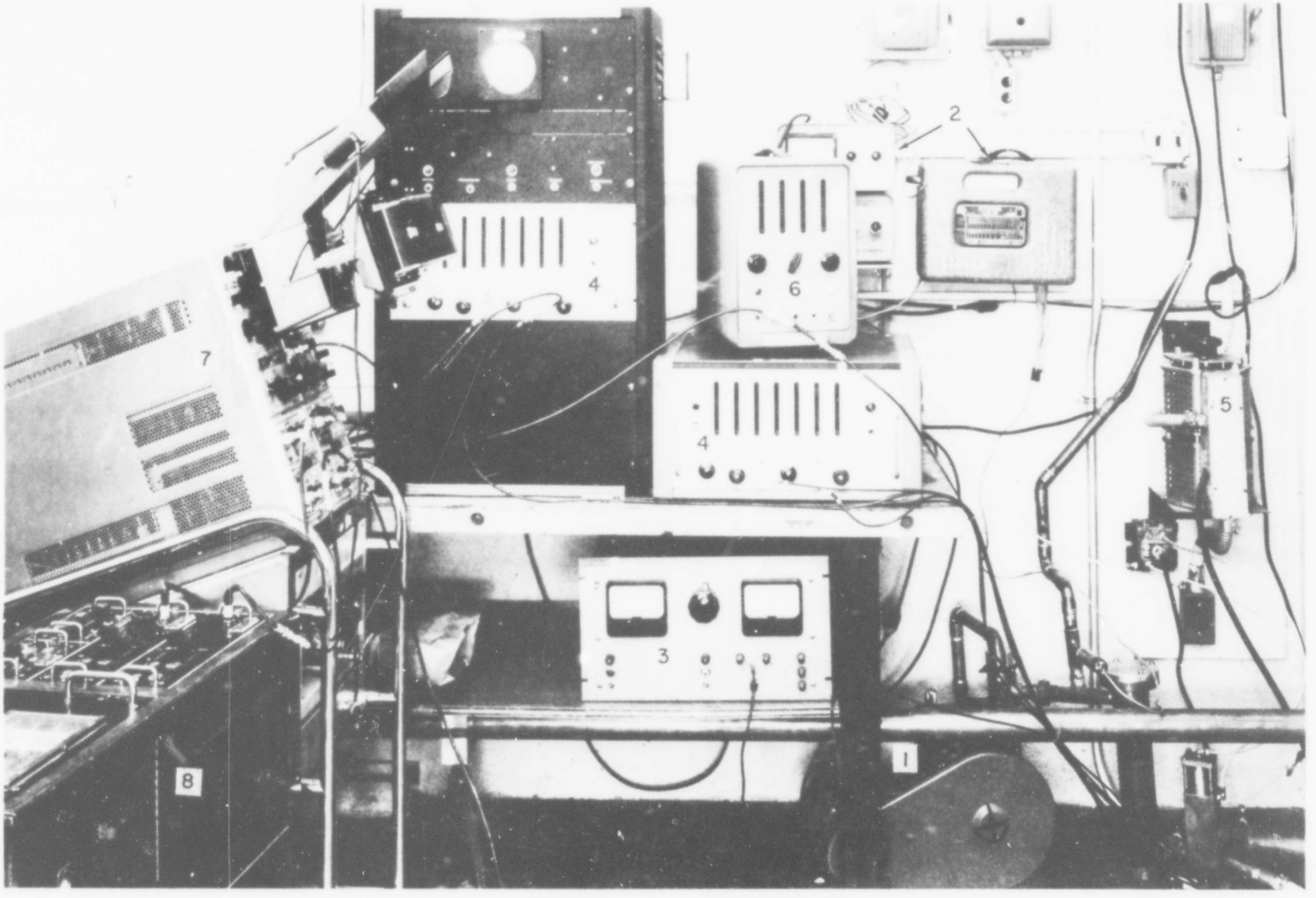

1120-65

Fig. 12 Associated Instrumentation.

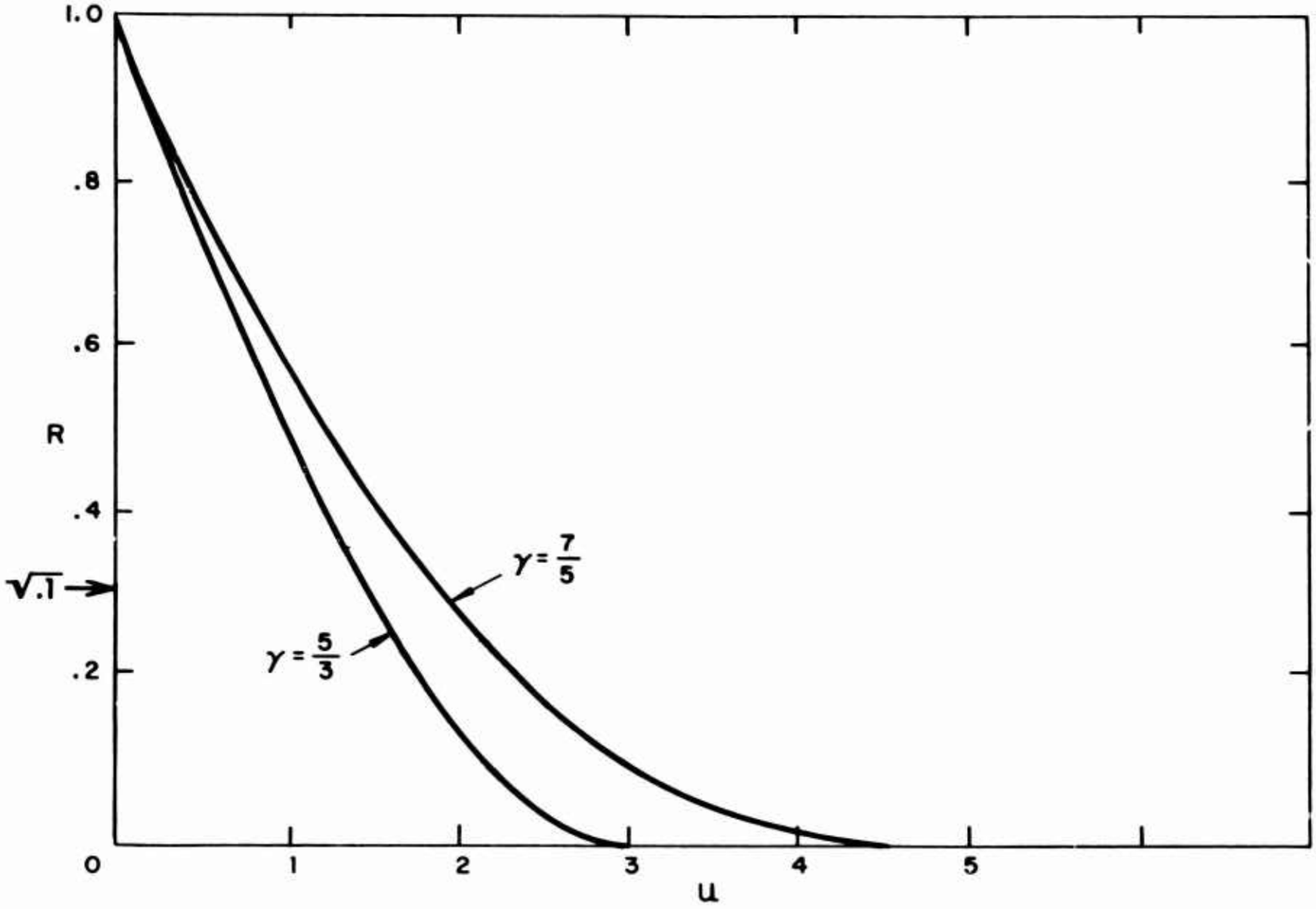

Figure 13. Efficiency versus nondimensional velocity.

Ideally, the maximum values of u would be 3 and 5 for γ's of 5/3 and 7/5. Practically, however, the efficiency R is down to $\sqrt{0.1}$ at about u of 1.5 and 1.9. This implies that a gun either 10 times longer or with 10 times the acceleration of the ideal gun would be needed to achieve these velocities. It therefore appears most attractive to concentrate on guns with as small a value of u as possible and impose a practical limit on u of about 1.

A plot of the attainable velocity for room temperature, air, and helium, constant diameter and infinite diameter chamber guns as a function of GL is presented in figure 14, where GL is the product of the peak acceleration G in the gun in g's and the length of the gun L in feet (from apx B and ref 9). From our present results (which will be discussed below) we expect that the gun performance for each gas would be in the hatched region between constant diameter and infinite diameter reservoirs.

These curves indicate the length of the gun needed if peak firing accelerations and muzzle velocity are chosen. For example, if one does not wish to exceed 1000 g in the gun but wants to obtain a velocity of 2500 ft/sec, GL is about 2×10^5 for helium and 12×10^5 for air, or L is 200 and 1200 ft, respectively. The ideal gun for such conditions need be only 100 ft long.

For helium gas used with the present gun, efficiency should always be greater than 85 percent up to 600 ft/sec (from fig. 13). With operating velocities of 3000 ft/sec the efficiency may drop below 60 percent making it desirable to counteract this by utilizing higher sound speed gas, ingenious devices, or more complex guns (ref 11).

Two assumptions implicit in the derivation of the performance of guns (apx B) are that friction does not slow the bird in the gun nor does any gas blow by the bird. In our initial tests one or two O-rings were used on the projectile to serve as a vacuum seal and to minimize blowby. The velocity when two O-rings were used indicated lower efficiency than expected while one O-ring results were only slightly more efficient. Furthermore, the velocity changed with the type of O-ring used as well as with different O-rings of the same lot. For this reason the O-ring was transferred from the bird to the gun, and the bird diameter was critically controlled to reduce blowby. Results with this system with an air driver gas indicate higher efficiency and greater reliability than achieved previously.

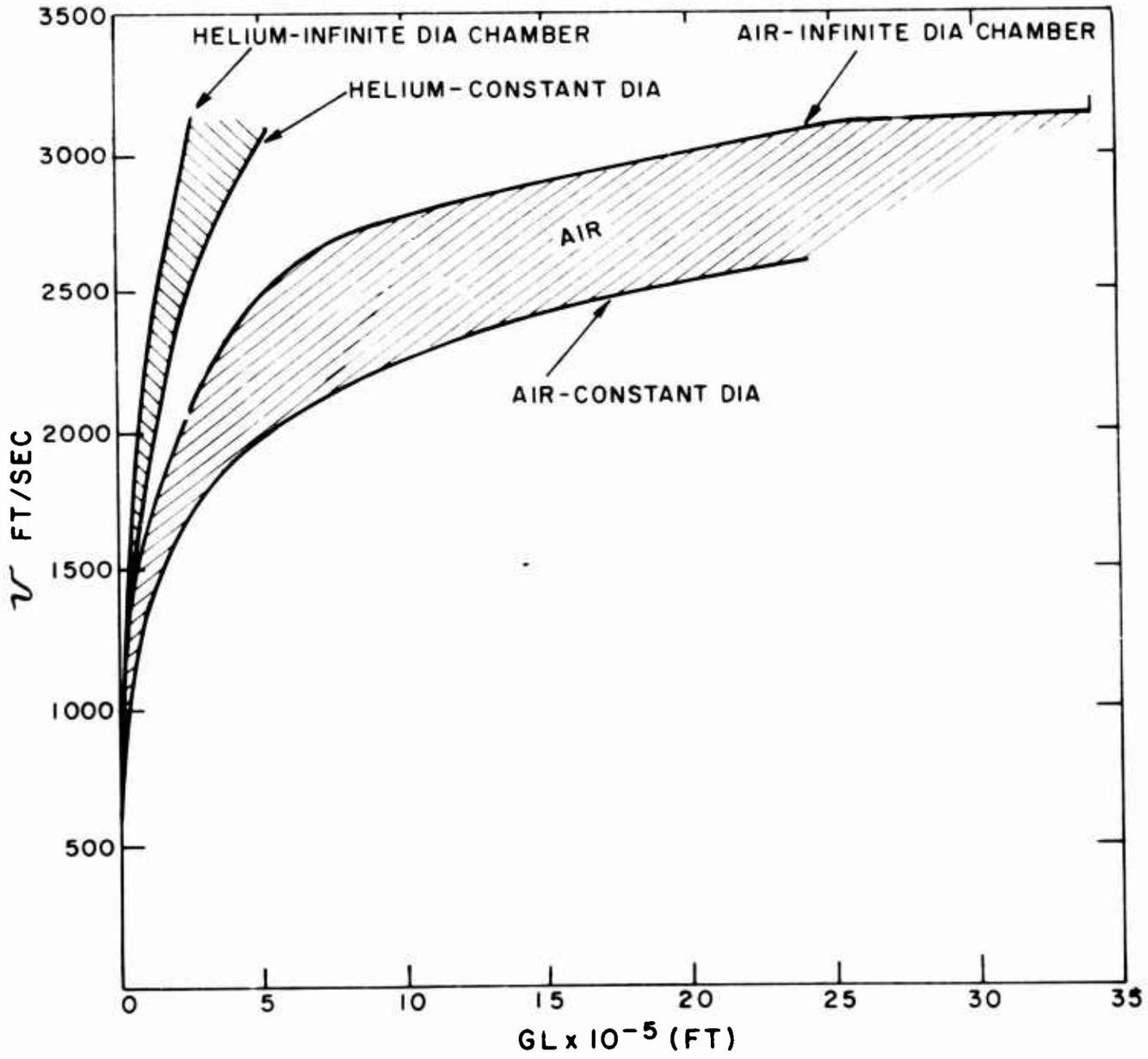

Figure 14. Bird velocity versus GL.

These results are graphically illustrated in figures 15, 16, and 17. In these the efficiency R of each shot was plotted as a function of a nondimensional parameter, X.* The upper and lower curves in each of these figures are for an infinite diameter reservoir and for a constant diameter gun, respectively which are discussed in appendix B. All of these data are for vacuum operation. Figure 15 represents the data taken with two O-rings on the projectile, figure 16 represents the data taken with one O-ring on the projectile and figure 17 represents data taken with the O-ring transferred to the gun. Even though in the last series the efficiency is significantly better, R still does not approach the theoretical values for the infinite diameter reservoir gun.

It was suspected that turbulence or poor flow characteristics in the vicinity of the breech, due to the abrupt change in area, might affect the bird velocity. A short nozzle was therefore added to smooth the transition, but this had no noticeable effect. The data in figure 17 include results with and without the nozzle.

Calculations indicate that friction and boundary layer effects at these low velocities have a small effect and that the loss in efficiency is more likely due to blowby. The gun is not of uniform diameter nor is it exactly circular. The ends of the gun measure 0.002 in. less than 2 in. whereas measurements of 0.002 in. over 2 in. have been made a few feet from the ends. Shots in figure 17 were made with projectiles of 0.005 in. less than 2 in. in diameter. At its worst this represents an area equivalent to a 1/4-in. diameter hole through the bird. Closer fitting birds will be fired in the gun, in an attempt to increase the efficiency. However, the fact that the gun barrel is not exactly straight can have an adverse effect on the results with closer fitting birds. Therefore, the results in figure 17 may be as good as can be obtained with this particular gun.

---

*$X = P_o A L / c^2 m_1$, where P_o is the initial gun pressure
A_o is the gun cross-sectional area
L is the gun length
m_1 is the mass of the bird.

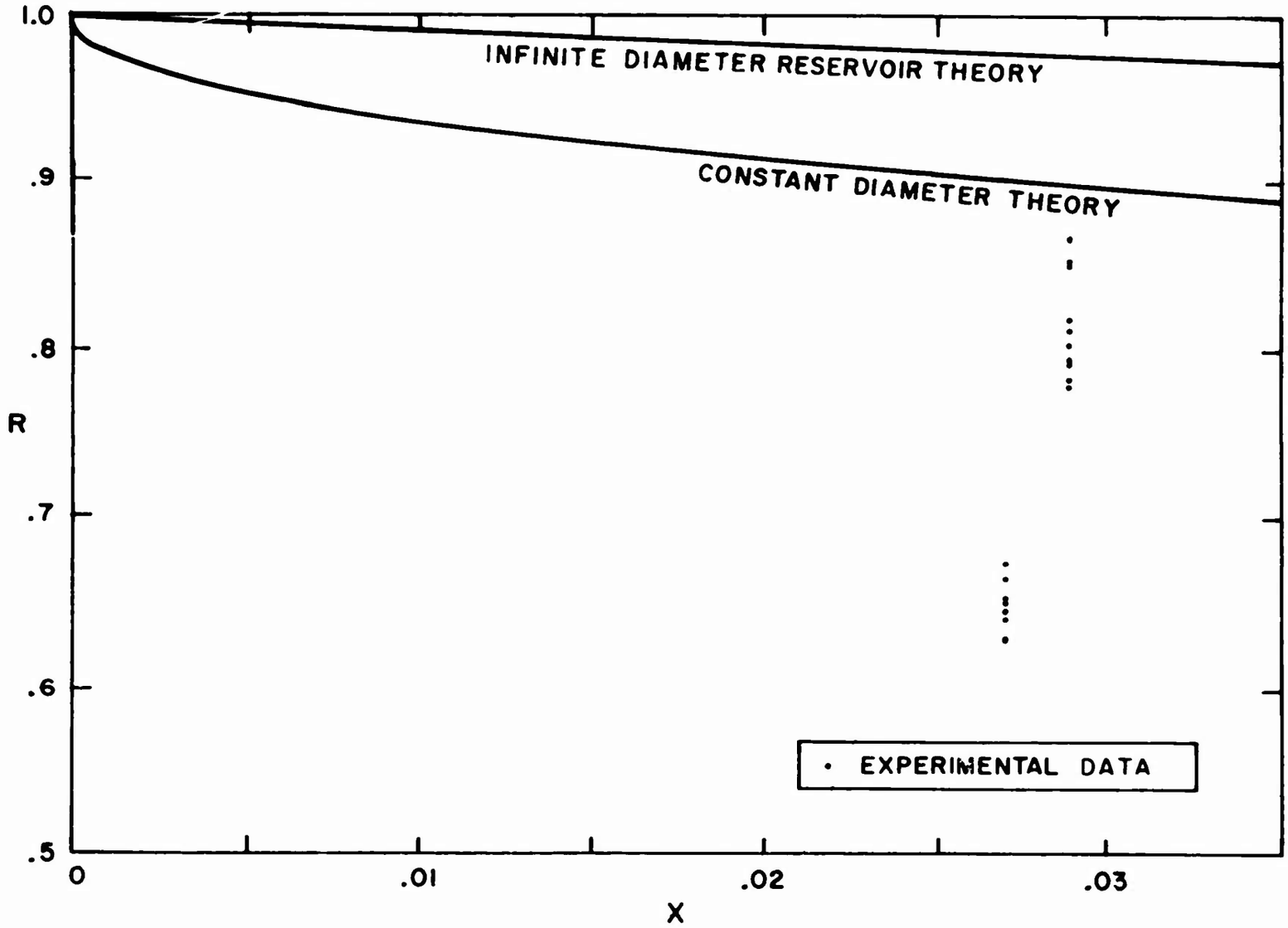

Figure 15. Efficiency versus nondimensional length. Air operation. Two O-rings on bird.

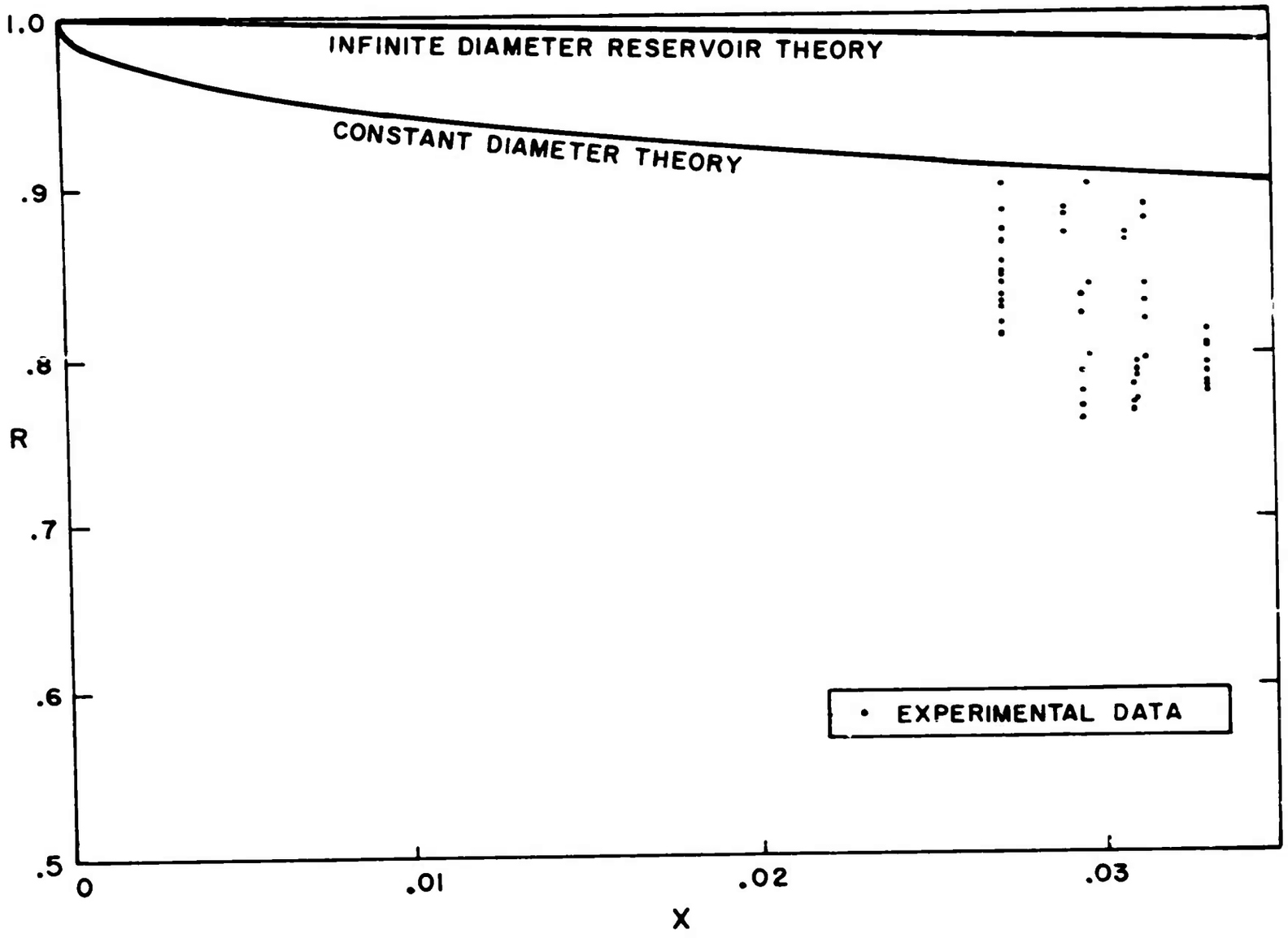

Figure 16. Efficiency versus nondimensional length. Air operation. One O-ring on bird.

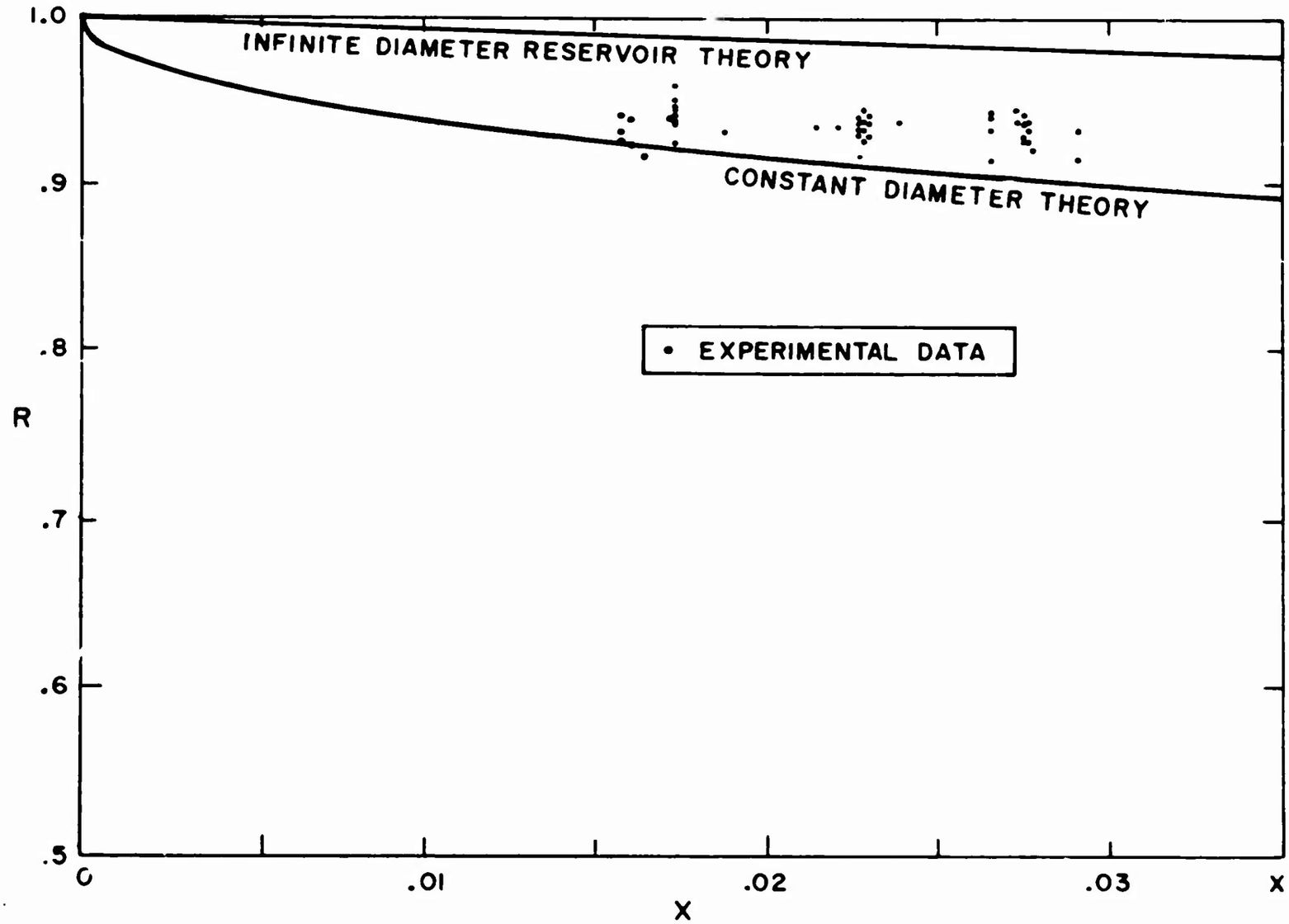

Figure 17. Efficiency versus nondimensional length. Air operation. O-ring in gun.

Figure 18 is another representation of the last series of data (O-ring in the gun). Here, the nondimensional velocity ($u = v/c$) is plotted as a function of nondimensional distance (X) for these data, for the constant diameter gun and for the infinite diameter reservoir gun.

Since the velocity is measured external to the gun, there is the possibility that there is a loss of momentum when the diaphragm is broken or due to air drag. However, the effect of air drag is negligible (appendix A) and the forces needed to break and accelerate the diaphragm are infinitesimal for heavy birds of the type used.

At least 30 shots have been made using helium and the driver tank. These shots (two O-rings, fig. 19; one O-ring, fig. 20) suffer in efficiency in the same manner as the air shots. One helium shot has been made since the O-ring was placed in the gun. There appeared to be little if any improvement in efficiency. Although no conclusions can be drawn from a single experiment, it should be noted that the efficiency could never exceed .92 for helium anyway because of the finite volume of the driver tank (appendix B).

4.2 Spin-Catcher

The spin-catcher with readout has performed well. It has been used in over 100 tests with no apparent deterioration of bearings or brushes. This is even more noteworthy since several bad impacts occurred immediately after changing over to this catcher*. The maximum impact acceleration measured has been 20,000 g. A new catcher is being designed with four segments to provide two additional readout channels. These channels may be used to monitor fuze component performance or perhaps, linear and/or angular acceleration upon impact.

4.3 Stopping Mechanism

The stopping mechanism has performed very satisfactorily in that very little data have been lost due to "bad"

---

*Due to an obstruction at the muzzle of the gun, several birds turned slightly before entering the catcher. The offset at impact was about 1/4 in. This caused considerable damage to the aluminum bird and bent the entrance end of the steel spin-catcher.

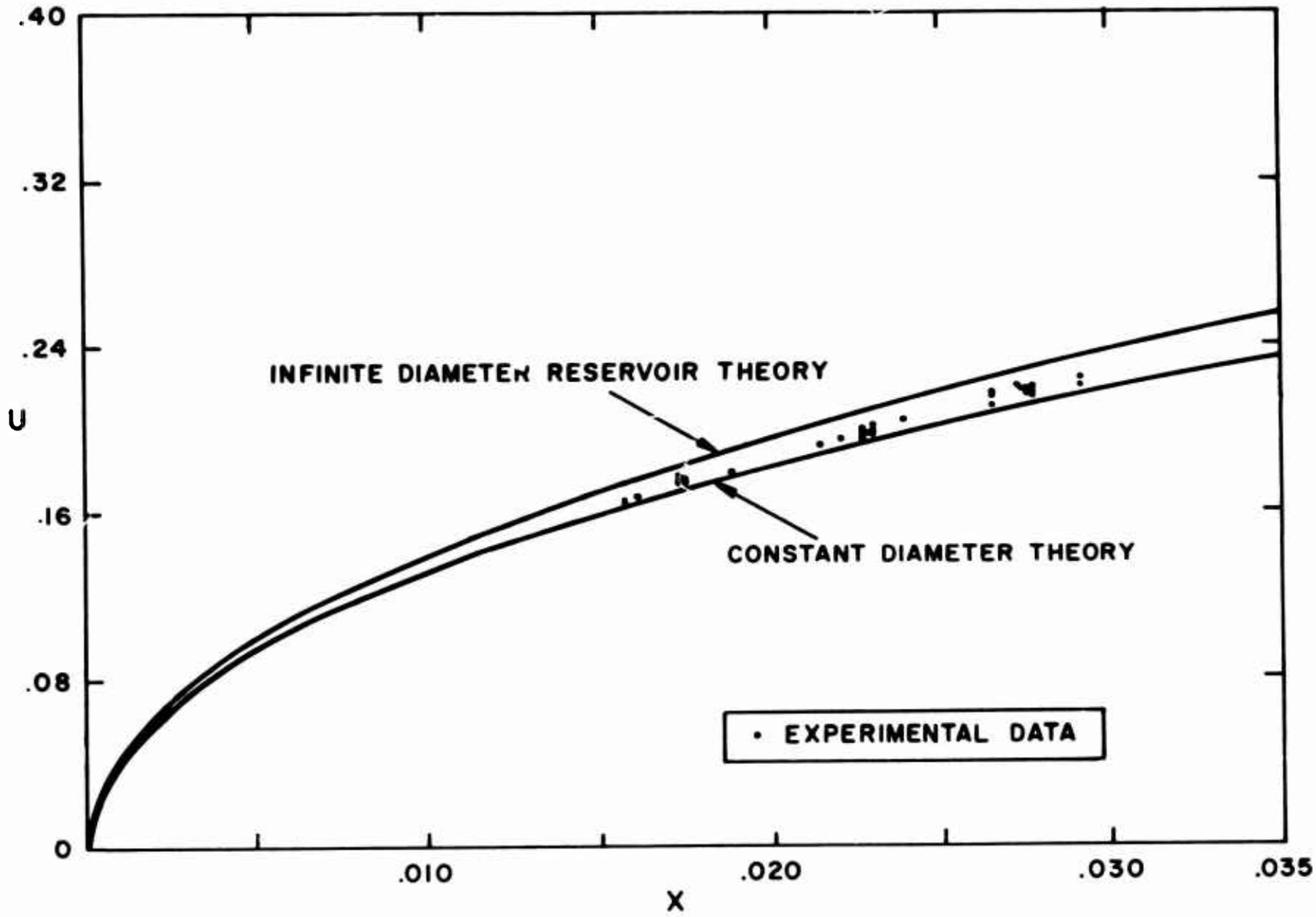

Figure 18. Nondimensional velocity versus nondimensional length using air driver.

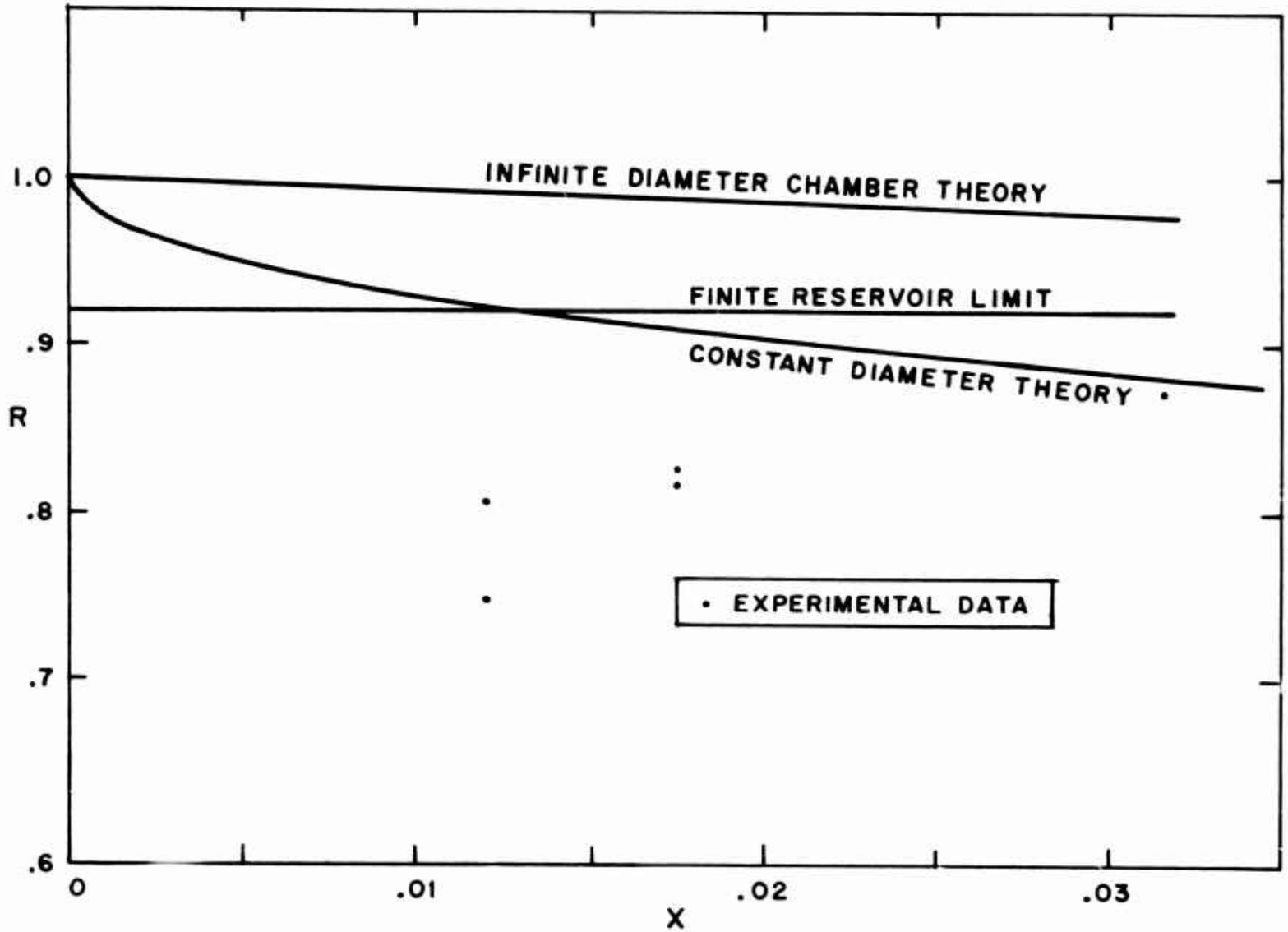

Figure 19. Efficiency versus nondimensional length. Helium operation. Two O-rings on bird.

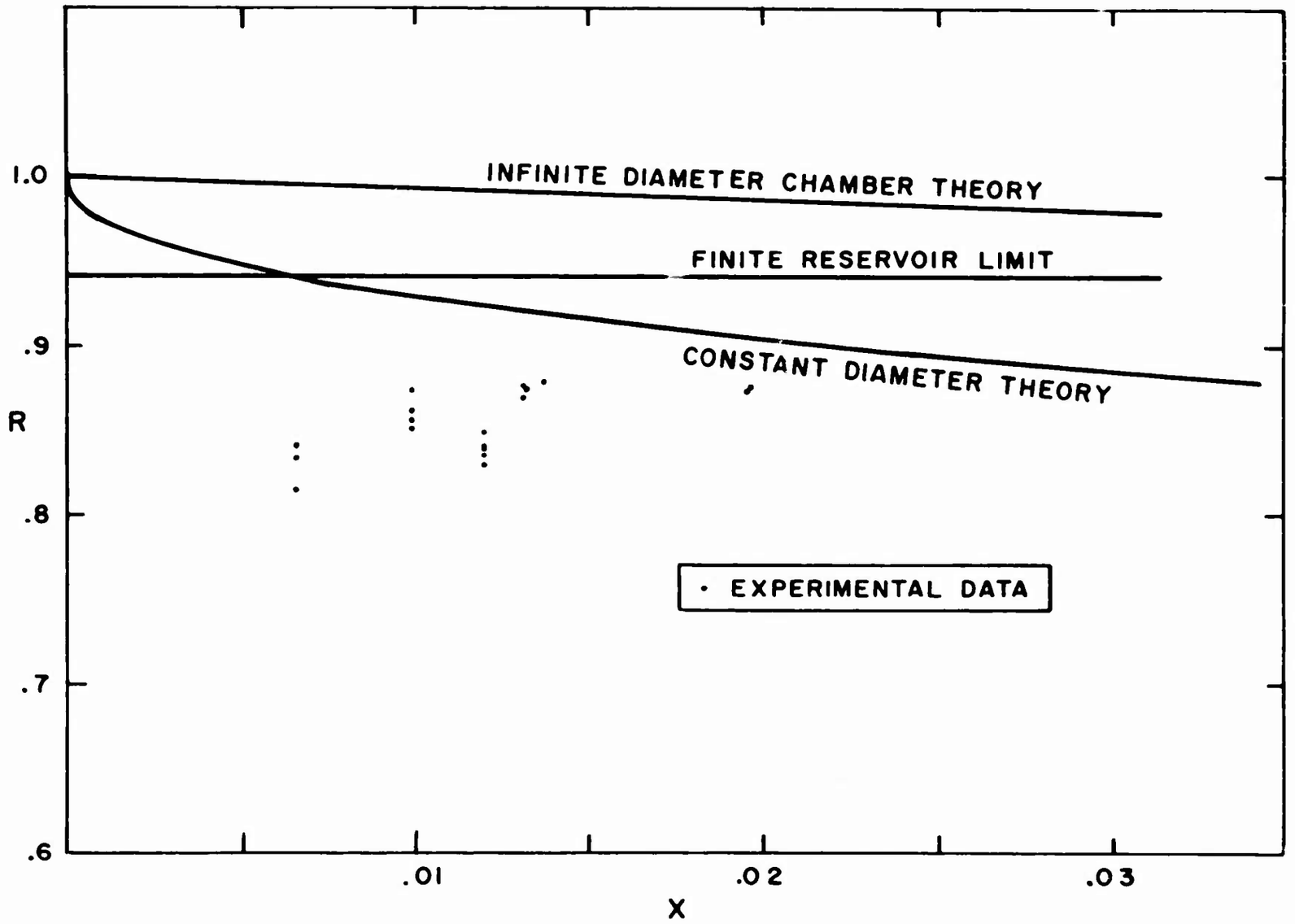

Figure 20. Efficiency versus nondimensional length. Helium operation. One O-ring on bird.

catches. However, how well we are simulating artillery firing requires deeper investigation. First let us consider how the system is behaving and then consider possible improvements.

4.3.1 Linear Deceleration

Our system initially consists of a moving bird, stationary wood and mem (fig. 4). We can make certain predictions about the system immediately after impact (if we neglect friction between the spin-catcher and these parts during impact). To simplify the analysis we shall assume that the mem and the wood act as a unit with an equivalent mass (m_2) composed of the sum of both.

Conservation of momentum and energy predict

$$m_1 v = m_1 u_1 + m_2 u_2 \tag{6}$$

$$E_o = 1/2\ m_1 v^2 = 1/2\ m_1 u_1^2 + 1/2\ m_2 u_2^2 + E_L \tag{7}$$

where

m_j is the mass
u_j is the velocity after impact
E_j is energy
$j = 0$ refers to initial condition
$j = 1$ refers to the bird
$j = 2$ refers to the wood-men combination

The inelasticity of the impact appears as a lost energy E_L. Unfortunately we have two equations with three unknowns u_1, u_2 and E_L.

If we knew the dynamic characteristics of the plywood, we might be able to derive an expression for the energy lost due to deformation. However, these characteristics did not appear in the literature; in fact one way to acquire such dynamic characteristics would be through this type of impact experiment.

We therefore had to take a more empirical approach to the problem. To do this it is preferable to rearrange equations 6 and 7. Implicit differentiation of equations 6 and 7 with respect to u_1 yields

$$du_2/du_1 = - m_1/m_2 \tag{8}$$

$$0 = m_1 u_1 + m_2 u_2 du_2/du_1 + dE_L/du_1 \tag{9}$$

or

$$dE_L/du_1 = m_1(u_2 - u_1) \tag{10}$$

This last expression equals zero when $u_2 = u_1$. This is usually referred to as a completely inelastic impact and it is seen (eq 10) that under this condition E_L is maximized. The maximum energy that may be dissipated (consistent with momentum conservation) E_M is therefore obtained from equations 6 and 7 when $u_1 = u_2$ and $E_L = E_M$.

$$E_M = E_o m_2/(m_1 + m_2) \tag{11}$$

We also obtain a minimum velocity for the mem u_L

$$u_L = m_1 v/(m_1 + m_2) \tag{12}$$

For the completely elastic situation,

$$E_L = 0$$

and the maximum velocity for the mem u_m is

$$u_m = 2m_1 v/(m_1 + m_2) = 2u_L \tag{13}$$

From the preceding, it can be shown that

$$E_L/E_M = u_2/u_L(2 - u_2/u_L)$$

The coefficient of restitution ϵ in terms of this notation would be

$$\epsilon = u_2/u_L - 1$$

$$E_L/E_M = (1 - \epsilon^2) \tag{14}$$

Values for the coefficient of restitution would suffice to completely determine the solution. However, the coefficient of restitution is a function of shape, impact

velocity and material (ref 12). This information is not available for this experiment. However actual experimental measurements of v, u_2, m_1 and m_2 produce the values listed below and from these we infer almost complete inelasticity, ($\epsilon \approx 0$).

E_L/E_M	No. of Shots	
1.000	34	105
.999	32	
.998	15	
.997	9	
.996	15	
.991 - .995	40	
.986 - .990	27	
.981 - .985	6	
All others	18	

Therefore, it has been assumed (where necessary) in reduction of the data that all impacts were completely inelastic.

The average deceleration of the projectile was computed (appendix C) based upon measured compressions of the wood and conservation considerations. It is important to realize that this is the deceleration that takes place during impact, which slows the bird down but does not necessarily bring it to rest. It is therefore necessary to postulate some lesser deceleration (due to friction), which stops the bird in the catcher. Estimates of this frictional deceleration based upon the location and velocity of the bird in the spinner after impact are typically 5 percent of the impact decelerations. The magnitude of this deceleration is strongly dependent upon how tightly the wood blocks fit in the spinner after impact. There has been no attempt to control this second deceleration.

The deceleration was also measured with copper-ball accelerometers, which measure peak acceleration when used in their operating range. Two different accelerometers were used in the tests, one with a natural frequency of 1021 cps and the other with natural frequency of 2185 cps. Because of this and the shape of the acceleration profile, there is no reason to expect both accelerometers to indicate the same acceleration. However, some correlation between computed and measured accelerations is to be expected if the results are at

all meaningful. There is considerable spread in the data for the higher frequency accelerometer. This is due in part to: (1) the smaller deformation of the copper ball because of the reduced mass of the accelerometer hammer; (2) acquisition of much of the higher frequency accelerometer data before it was realized that plywood quality had to be selected and controlled carefully; and (3) less deformation of the wood stack at the higher g's (shorter stopping distance). Where only the later data are investigated, the spread appears to be considerably reduced. Figure 21 presents these results as a plot of peak acceleration from the copper-ball measurement versus computed average acceleration. In this graph the data have been presented for the 2185-cps accelerometer by averaging the average accelerations over a small peak acceleration interval, while for the 1021-cps accelerometer the peak accelerations were averaged over a small average acceleration interval. This was done to demonstrate that for the high frequency accelerometer most of the error is probably due to errors in computation of the average deceleration while for the low frequency accelerometer where more care and control were exercised over the plywood, the spread is most likely due to inaccuracy of the copper-ball accelerometer. Straight least square lines through the origin have been drawn which indicate that the peak g at 2185 cps is about 2.3 times the average, while at 1021 cps it is about 1.4 times the average. Behavior of this type has been observed in other tests (ref 4) in which the actual acceleration pulse is of complex shape.

4.3.2 Angular Acceleration

Aside from the high-speed photographs mentioned in section 2.3, there has been little effort to ascertain the details of the angular acceleration profile. The only quantitative results have been obtained by noting how many times a power supply signal changed polarity in the output. This change in polarity is due to a relative rotation of the bird and the catch tube which causes the contacts on the bird to slip from one segment to another. There has been an average of one change of polarity per shot for those shots on which readout was obtained. However, different birds (different moments of inertia), different linear velocities, and different angular velocities have been used and there are insufficient data

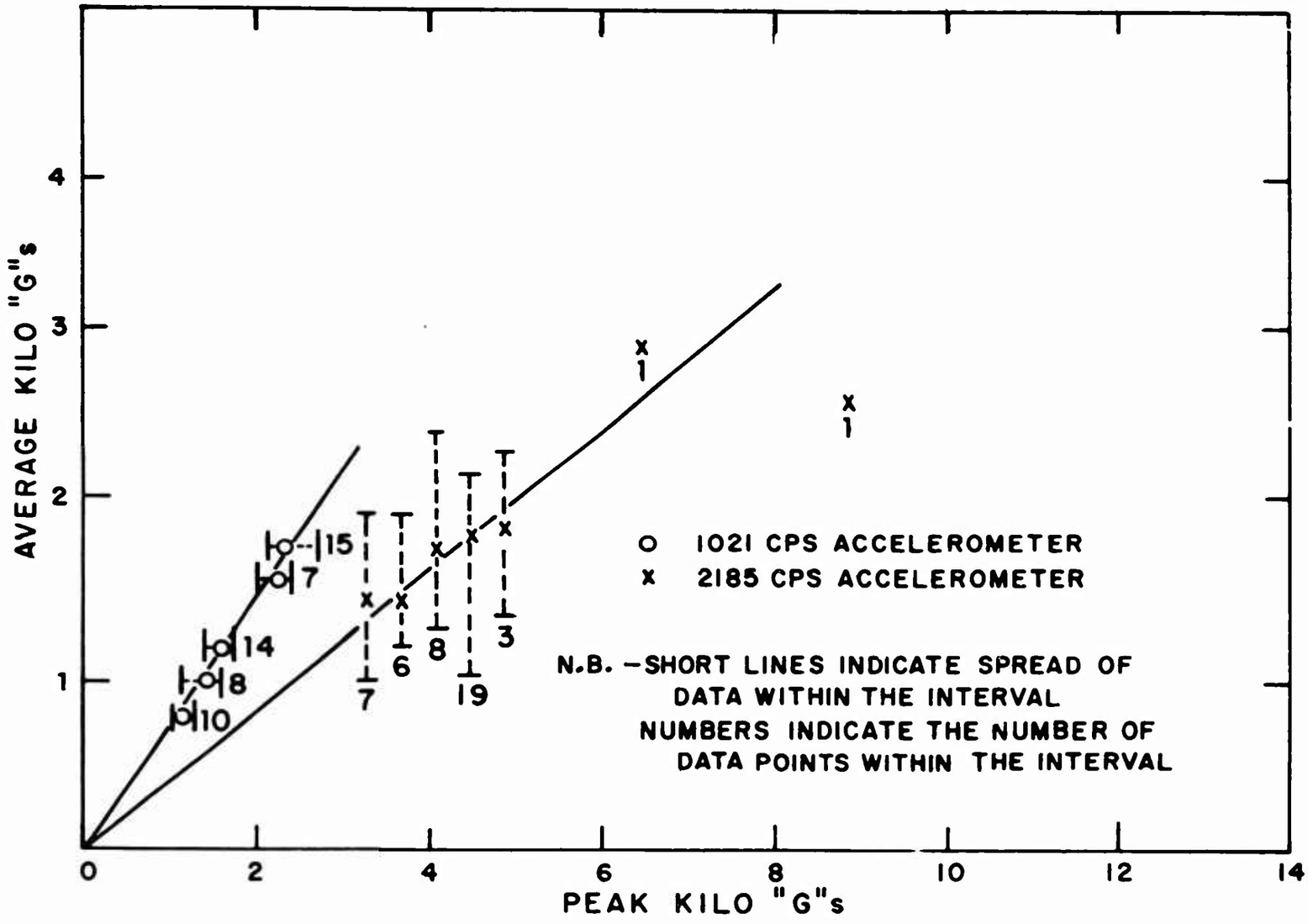

Figure 21. Computed average acceleration versus measured (copper ball) peak acceleration.

to make meaningful correlations. The four-segment catch-tube will provide more quantitative results since the signal will be advanced every 90 deg rather than every 180 deg.

4.3.3 Improvements in Stopping Mechanism

The equipment is performing qualitatively as required. We are achieving g levels, angular velocities, and angular accelerations consistent with values expected in the field. However, more information of a quantitative nature is required regarding the actual time profiles of these phenomena and an evaluation must be made of exactly which of these phenomena are of significance for fuze performance. The major defect in the present equipment is the low velocity imposed by space limitations (see sec 2.1). Velocities are only 20 percent of field values at the high accelerations. At higher velocities if the peak decelerations are kept constant, the duration of the decelerations will be increased. This necessarily means a change in the deceleration-frequency spectrum of the setback pulse, which will increase the low frequency components. The desirability of increasing these low-frequency components should be thoroughly investigated, since any simulation of the type described herein will have to be greatly expanded in terms of space and expense. Therefore, it is proposed that the following be undertaken: (1) an analysis of the mechanical frequency response of fuzes to determine those frequencies that should be most realistically simulated; (2) based on (1) choose a desired (minimal) acceleration time profile; (3) re-evaluate the impact velocity and stopping mechanism; (4) demonstrate the feasibility of a proper stopping mechanism; and (5) construct a gun of sufficient length to keep the acceleration-to-deceleration ratio favorable.

4.4 Readout

The sample readout in figure 22 shows the result obtained when a 535-gm bird containing a 1.3-v mercury cell was fired at a velocity of 432 ft/sec into the catcher. In the uppermost trace is the output of a variable reluctance pickup used to measure the angular velocity of the spinning tube; a characteristic noise signal appears at entry of the projectile due to vibration of the catcher and is assurance that the oscilloscope triggered at the proper time. The pips appear each time a flat on the tube passes the pickup.

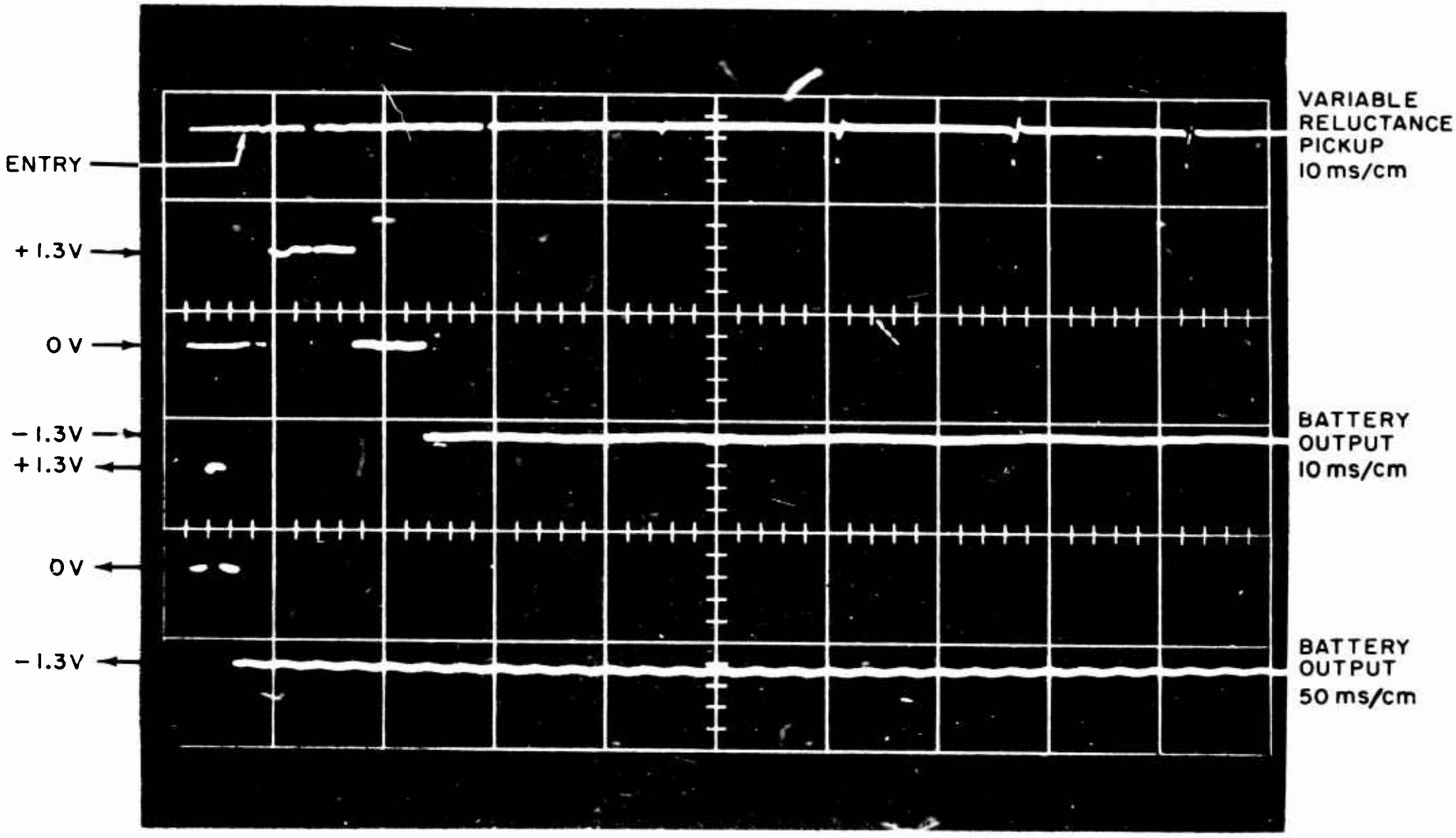

1227-66

Fig. 22 Sample Readout Picture.

The middle trace shows the battery voltage at the scope as a function of time. The voltage at entry is zero, jumps to 1.3 v shortly thereafter, returns to zero, then goes to -1.3 v. The entire sequence happens within one revolution of the spinner, spinning at 65 rps.

Careful inspection reveals some breaking of the circuit during the positive portion of the signal. This is due to a contact on the bird leaving a segment of the spinner. This type noise or loss of signal may be alleviated through redundancy of contacts as used in brush systems. The relatively long time between changes of polarity of the signal is not typical. In this particular shot the bird was moving very slowly at crossover.

The lowest trace contains the same information as the second but on a time base of 50 ms/cm. The modulation of the signal, which is at the spinner frequency, is apparently due to resistance of the brushes. This signal will hopefully be reduced in the next model by using a better brush system. The brush noise is greatest at the high spin rates, although successful readout has been obtained over the entire range of operation. Signals obtained on chart recorders have provided output for times in excess of a minute.

The bird contact system used on this test is described in reference 6; however, somewhat simpler designs are being investigated, which may perform as well.

5. CONCLUSION AND RECOMMENDATIONS

A system has been designed and built for testing fuze components in an environment simulating the interior ballistic accelerations of artillery weapons. The simulator has performed extremely well within the limits imposed by (1) available space, (2) state-of-the-art of rotating devices, and (3) time.

While evaluating this test facility, a new fuze power supply requiring both angular and linear acceleration for proper operation, was tested and the results utilized for engineering redesign of the battery. The development of this battery, which shows great promise, would otherwise have been suspended because of the difficulty and cost of field testing.

In light of the demonstrated feasibility of the concept, the demonstrated use of this type of facility for tests not practical otherwise, and its anticipated savings in time and money, it is

recommended that the following course of action be taken to maximize its value to the fuze scientist and to the services.

(1) An analysis should be made of the effects of forces on fuzes or components to determine what are the more important forces to be simulated (see sec 4.3.3).

(2) A determination should then be made of whether an improvement in the current design could be achieved (4.3.3). It is very likely that the most significant improvement would be accomplished by prolonging the deceleration time.

(3) Concurrently, a survey should be made of the sizes and environments of artillery fuzes now under development or expected to be developed in the next 10 years to establish realistic goals for the properties of a more advanced simulator.

(4) Assuming that the results of the above bear out the hypothesis that both longer stopping distances and a larger diameter are needed, investigations will have to be made into the state-of-the-art of long guns (sec 4.1) and high-speed bearings.

(5) The possibility of using telemetry at high rotational velocities should be investigated.

(6) Based upon the results of the preceding, appropriate action should be taken to construct a facility that will provide the best simulation.

6. REFERENCES

(1) U.S. Department of Commerce, National Bureau of Standards, Air Gun Building, 1952.

(2) De Vost, V. F., NOL Copper-Ball Accelerometers, Nav Ord Report 6925, November 1960.

(3) Zhmur, A. S., et al, Single Action Accelerometers, Mechanical Measurements, 12, 997, 1963.

(4) De Vost, V. F., NOL Copper-Ball Accelerometers, NOL TR 63-279, February 1966.

(5) Energy Absorbing Characteristics of Several Materials, Report SCTM 284-57 (51), Sandia Corp., Livermore, California, 1960.

(6) Martin, H., Construction Details of HDL Artillery Simulator (Prototype), HDL Report (in preparation).

(7) Appendix to—Brody, P. S., Strong Shock Waves in "Polled" Barium Titanate Ceramic Elements, DOFL Report No. TR-869, 20 October 1960.

(8) Shapiro, A. H., The Dynamics and Thermodynamics of Compressible Fluid Flow, Ronald Press, New York, 1953.

(9) Seigel, A. E., The Effect of the Optimum Chambrage on the Muzzle Velocity of Guns with a Qualitative Description of the Fundamental Phenomena Occurring During Gun Firing, Nav Ord Report 2691, October 1952.

(10) Seigel, A. E., Dawson, V. C. D., Results of Chambrage Experiments on Guns with Effectively Infinite Length Chambers, Nav Ord Report 3636, April 1954.

(11) Seigel, A. E., The Theory of High-Speed Guns, AGARDograph 91, NATO May 1965.

(12) See for example, Goldsmith, Werner, Impact, Edward Arnold Ltd., London, England, 1960.

BLANK PAGE

APPENDIX A.—TRAJECTORY OF BIRD FROM MUZZLE TO SPIN CATCHER

I shall first demonstrate that there is an insignificant change in velocity due to drag in the free flight between the gas gun muzzle and the spin-catcher and then compute the drop distance due to gravity based on this conclusion.

Assume a maximum drag coefficient C_D of 2*; then the drag force D would be

$$D = 2(1/2\ \rho v^2\ A) \qquad \text{(A-1)}$$

where ρ is the density of air, v is the bird velocity, and A is the projected cross sectional area of the bird. The drag deceleration, $\dot{v}$ is therefore

$$\dot{v} = -\ \rho\ A/m_1\ v^2 \qquad \text{(A-2)}$$

which integrates to

$$\Delta v/v = e^{-(\rho A/m_1)\chi} - 1 \qquad \text{(A-3)}$$

where m_1 is the mass of the bird, χ is the distance travelled in inches and Δv is the change in bird velocity.

For

$$\rho = 4.65 \times 10^{-5}\ \text{lb/in.}^3$$

$$A = 3.14\ \text{in.}^2$$

$$m_1 = 1\ \text{lb (minimum)}$$

$$\Delta v/v = e^{-1.46 \times 10^{-4}\chi} - 1$$

Therefore for travel distances of less than 5 ft there is less than a 1 percent loss of velocity due to air drag. In the present facility χ is always less than 5 ft and therefore air drag is negligible.

---

* See for example, Tietjens, O.K.G., Applied Hydro- and Aeromechanics, McGraw Hill, 1934.

A nonspinning vehicle travelling horizontally (without drag) will follow a trajectory determined by

$$\chi = vt \tag{A-4}$$

$$y = 1/2\ gt^2 \tag{A-5}$$

where t is time, y is vertical distance measured down, and g is the acceleration due to gravity. Hence

$$y = g\chi^2/2\,v^2 \tag{A-6}$$

Figure 3 shows drop distance y versus velocity v with travel distance χ as a parameter.

APPENDIX B.—GAS GUN PERFORMANCE

The gas gun used in this facility does not readily lend itself to analytic mathematical analysis. Although the Riemann method of characteristics can be used to obtain the performance theoretically, little insight is gained as to the physics of the problem. I shall therefore present two relationships for such guns, one an upper and the other a lower bound. I will also discuss a representative treatment of a gun of this type by Seigel (ref 9). From these, all the salient features of the device will be available.

First, let us consider the velocity obtainable in a gas gun computed on the basis that the gas pressure is always uniform throughout the gun (no wave structure) and that the kinetic energy of the gas is negligible. This establishes an upper bound for the velocity. In this case (see fig. 23) assuming isentropic conditions we may write

$$PV^{\gamma} = P_o V_o^{\gamma} \qquad \text{(B-1)}$$

where

P_o = initial pressure

P = instantaneous pressure

V_o = initial volume (volume of tank with bird at $\chi = 0$)

V = instantaneous volume = $V_o + A\chi$

γ = ratio of specific heats for the particular gas used

γ = 7/5 for diatomic gases (air)

γ = 5/3 for monatomic gases (helium)

A = cross sectional area of gun

χ = instantaneous position of bird.

The acceleration $\dot{v}$ of the bird is

$$\dot{v} = \frac{PA}{m_1} \qquad \text{(B-2)}$$

where m_1 is the mass of the bird.

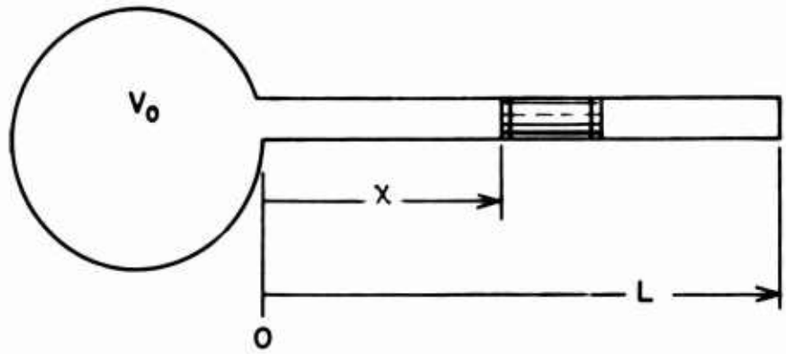

Figure 23. Gun coordinate system.

Therefore

$$\dot{v} = a_o(1 + A\chi/V_o)^{-\gamma} \tag{B-3}$$

where

$$a_o = \frac{P_o A}{m_1} \tag{B-4}$$

is the initial acceleration. Since

$$\dot{v} = v\, dv/d\chi \tag{B-5}$$

a first integral is immediately obtainable

$$v^2 = 2a_o V_o[1 - (1 + A\chi/V_o)^{(1-\gamma)}]/(\gamma - 1)A \tag{B-6}$$

or

$$v_m^2 = 2a_o V_o[1 - (V_o/V_F)^{(\gamma-1)}]/(\gamma - 1)A \tag{B-7}$$

where

v_m is the muzzle velocity computed in this manner

$V_F = V_o + AL$ = final volume of the gun

L = length of gun barrel.

For this gun

$A = 3.14$ in.^{2}

$L = 32.4$ ft

Helium Firing	"Vacuum" Operation (Room Air)
$V_o = 3.2\ ft^3$	$V_o \approx \infty$
$\frac{AL}{V_o} = 0.22$	$\frac{AL}{V_o} \approx 0$

and

$\frac{V_F}{V_o} = 1.22$	$\frac{V_F}{V_o}$ 1

This equation (B-7) sets the maximum velocity for such a gun (v_m). We would like to obtain also a measure of performance of the gun. Such a quantity, for our use, would be the ratio (R) of the muzzle velocity (v_m) of the gun to the ideal velocity ($\sqrt{2a_oL}$). In the ideal gun this number would be unity. Since

$$R_u = v_m/\sqrt{2a_oL} \qquad \text{(B-8)}$$

$$R_u^2 = [1 - (V_o/V_F)^{(\gamma-1)}]\ V_o/AL(\gamma-1) \qquad \text{(B-9)}$$

where the subscript u indicates an upper bound. The efficiency based on the model of such a gun does not depend upon the velocity, but only on the initial and final volume. For our gun with helium in the driver tank, $R_u = 0.92$. When used with room air as the driver, R_u approaches 1 and v_m^2 approaches $2a_oL$.

The other readily soluble case is the effectively infinite length driver-constant area gun (ref 7). Because the driver section of the gun is much greater in diameter than is the barrel, this gun should perform better than the result presented below; therefore the following results should represent minimum accelerations ($\dot{v}_L$) and velocities (v_L).

From reference 7

$$\dot{v}_L/a_o = [(1-(\gamma-1)u/2]^{2\gamma/(\gamma-1)} \qquad \text{(B-10)}$$

and

$$(\gamma+1)X/2 = 1-[1-(\gamma+1)u/2][1-(\gamma-1)u/2]^{(\gamma+1)/(1-\gamma)} \qquad \text{(B-11)}$$

where

$$u = v_L/c$$

$$X = a_o\chi/c^2$$

and c is the speed of sound of the driver gas. Therefore

$$R_L = \frac{\gamma+1}{4} \frac{u^2}{1 - [1- \frac{(\gamma+1)u}{2}][1- \frac{(\gamma-1)u}{2}]^{(\gamma+1)/(1-\gamma)}} \qquad \text{(B-12)}$$

where subscript L indicates the lower bound.

The third model as described by Seigel (ref 9) involves computation of effects of wave reflections from the section containing the change in area. Unfortunately such computations are tedious when performed by graphical means, and when solved on digital computers the effects of varying parameters are obscured. Seigel has made quite a thorough investigation of the effect of increased area in the driver section of the gun (chambrage, ref 8,9,10). The effect of chambrage is to maintain the pressure behind the bird at a high value. I have used some of his results for $\gamma = 7/5$ for computation of infinite chambrage and computed similar curves for $\gamma = 5/3$ (figs. 14-20). The results of these computations are significant for "vacuum" operation of the gun as an upper bound on the efficiency. The operation with helium is still in a region where it is limited by the finite volume of the driver tank.

APPENDIX C.—COMPUTATION OF AVERAGE DECELERATION OF THE BIRD

To compute the average deceleration of the bird during impact, it is necessary to know the initial velocity of the bird (v), the velocity after impact (u_1), and the distance over which the impact takes place.

If friction is excessive and the exit velocity of the mem u_2 is less than the ideal minimum velocity, u_L, based upon conservation conditions (4.3.1, eq 10), the assumption is made that the velocity of the bird after impact u_1 is equal to u_2. However, if u_2 is greater than u_L the velocity of the bird after impact is computed from momentum conservation.

From calculations of the ratio of the energy dissipated during impact to the maximum allowable dissipation (4.3.1, table I) it has been shown that the collision is virtually completely inelastic. This implies that only small amounts of energy stored in (recoverable) deformation of the wood is returned to the bird or mem during impact.

If we assume that the plastic deformation takes place at constant force or constant average acceleration, we may compute the impact distances in terms of the dimensions of the wood before and after impact. If we draw the life lines of the system during impact (fig. 24), we note that acceleration takes place during the dashed portions of the trajectories. This occurs during the time that the wood compresses from its original length L_O to its minimum length L_M and then expands to its final length L_F. We can express these lengths in terms of the X as follows:

$$L_O = X_4 - X_1 \tag{C-1}$$

$$L_M = X_5 - X_2 \tag{C-2}$$

$$L_F = X_6 - X_3 \tag{C-3}$$

The (constant) force, F, times the distance over which it acts must represent the change in kinetic energy of the bird or mem since it is assumed no deformation of these bodies occurs. Therefore for the bird

$$F(X_3 - X_1) = E_1 - E_3 \tag{C-4}$$

and

$$F(X_2 - X_1) = E_1 - E_2 \tag{C-5}$$

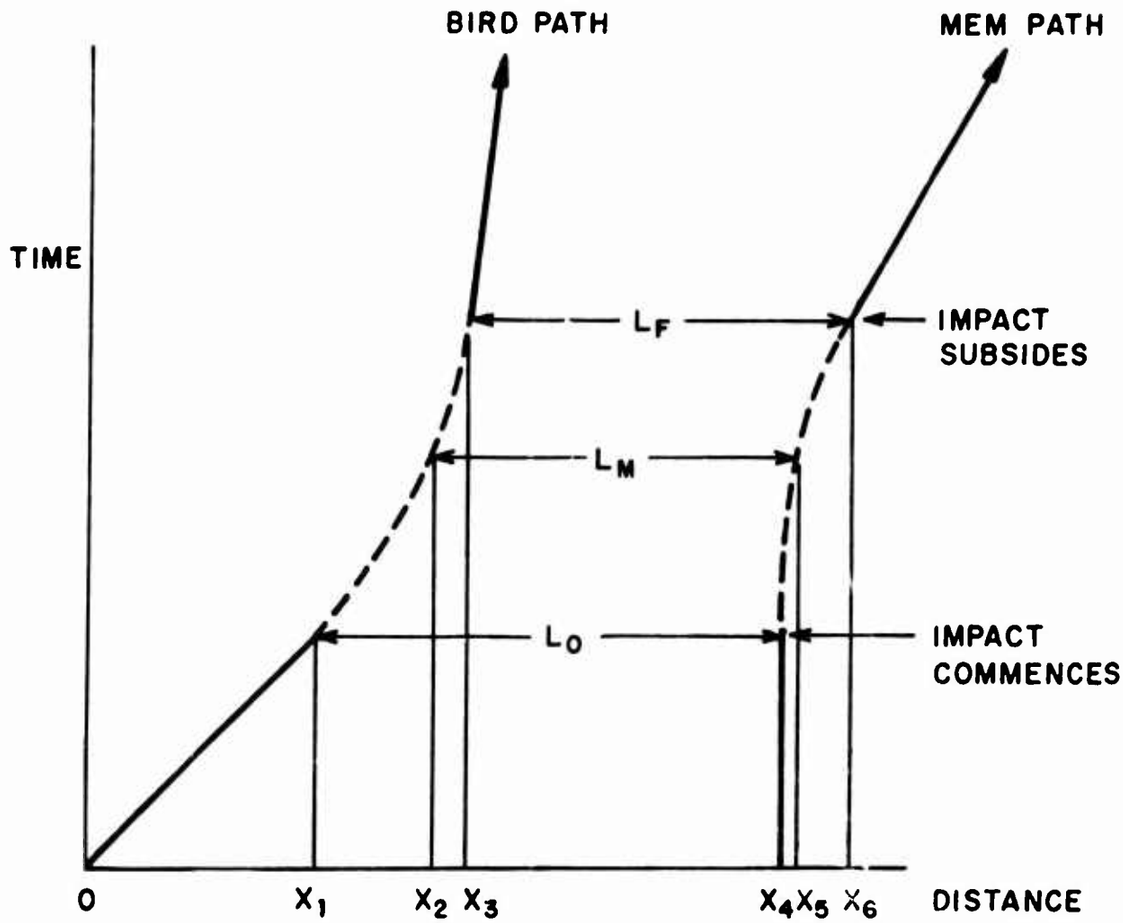

Figure 24. Life lines during impact.

while for the mem since $E_4 = 0$

$$F(X_6 - X_4) = E_6 \tag{C-6}$$

$$F(X_5 - X_4) = E_5 \tag{C-7}$$

Energy conservation implies

$$E_1 = E_a + E_6 + E_L \tag{C-8}$$

where E_L is the energy lost in deformation of the wood. Energy conservation also implies

$$E_1 = E_2 + E_5 + E_M \tag{C-9}$$

where E_M is the energy both lost and/or stored in the wood at maximum compression. E_M may be shown to be equivalent to the (maximum) amount of energy dissipated in purely inelastic impact.

Substituting (C-1) through (C-7) in (C-8) and (C-9)

$$E_L = W(L_o - L_F)\ G \tag{C-10}$$

$$E_M = W(L_o - L_M)\ G \tag{C-11}$$

where $F = WG$, $W = mg$ = weight of bird, and G = average acceleration of bird in "g's."

Either (C-10) or (C-11) could be used to determine the average acceleration G if we knew the energy loss and the dimensions of the wood before and after impact.

The energy lost during impact, E_L, and the maximum amount that could be lost, E_M, as pointed out in the main text, can be determined from velocity measurements and the masses. However, the final length of the wood, L_F, is not readily measured because the wood exhibits some delayed elasticity (or memory). By the time the wood is measured it has recovered some of its lost length.

A simple experiment to determine the relation between net strain σ_n and gross strain σ_g was performed. Single wood blocks were rapidly compressed to a specific gross distance by using adjustable stops in an arbor press. Each block was measured within 30 sec after compression and again subsequently (between 10 and 15 min later). The results are shown in figures 25 and 26. Since the measurements of the net deformation of the wood are usually made about 10 min after a firing, the results in figure 26 were empirically fit by an analytic expression

$$\sigma_g = 1.14\ \sigma_n + 0.085(1 - e^{-11\sigma_n}) \tag{C-12}$$

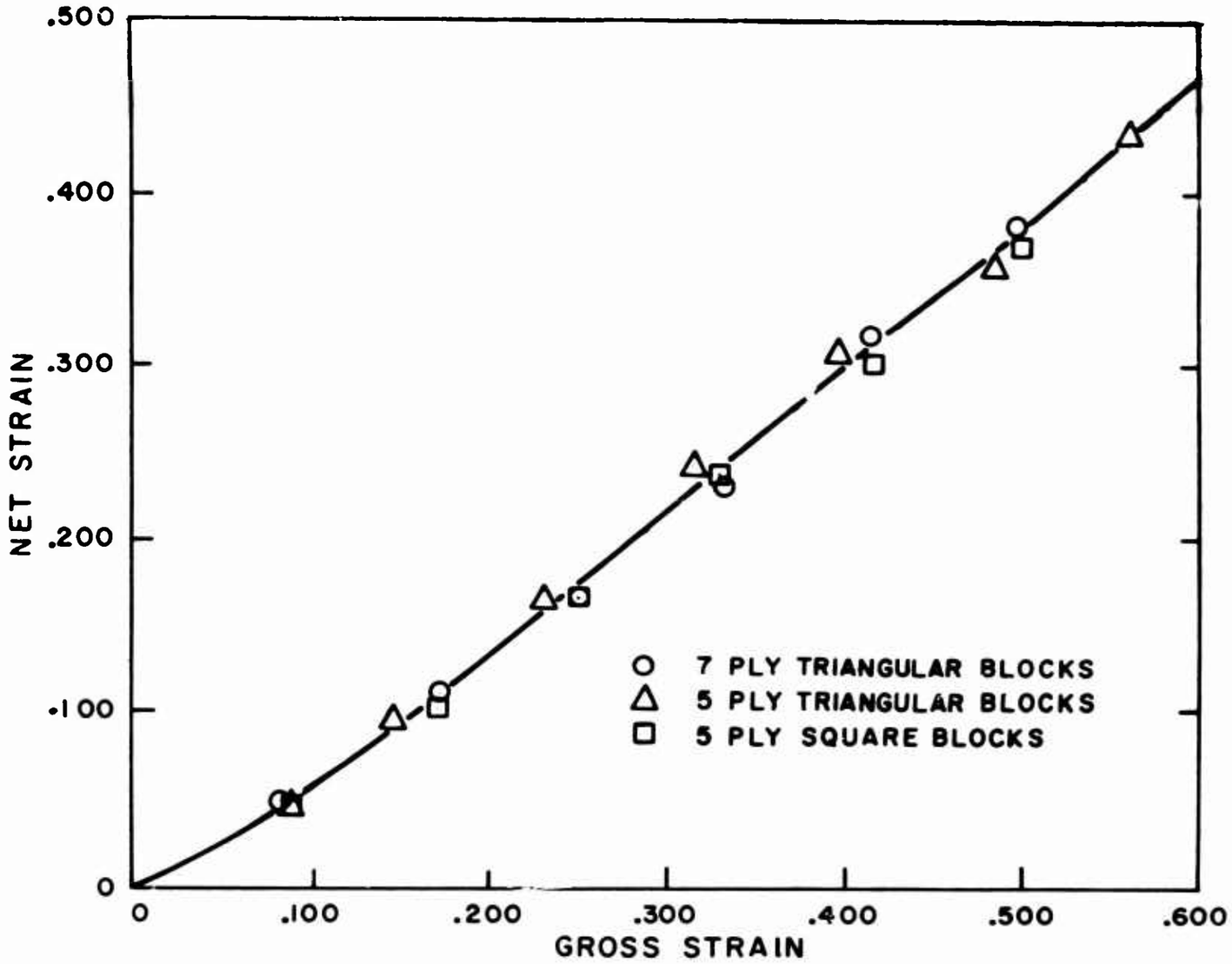

Figure 25. Net versus gross strain for 3 types of plywood (immediate).

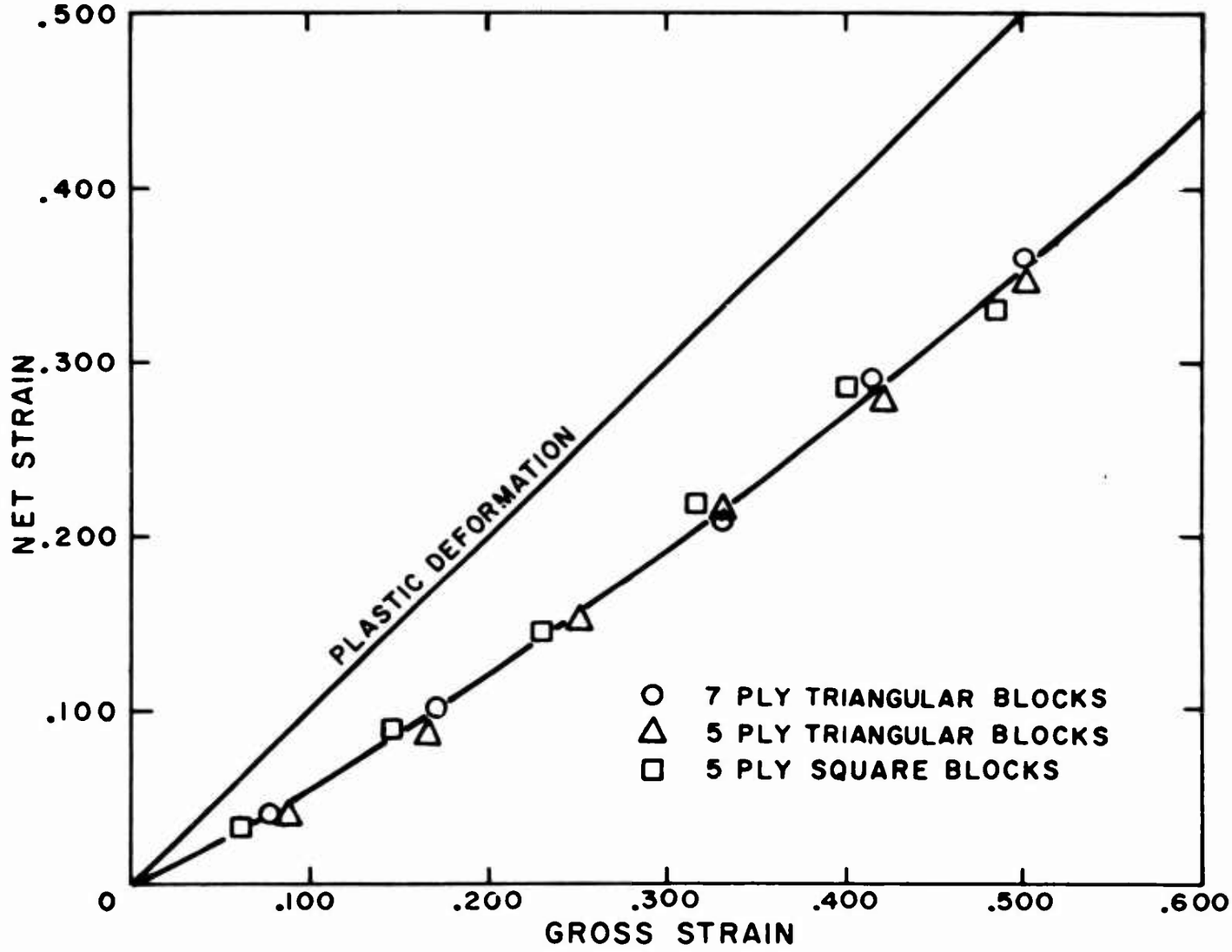

Figure 26. Net versus gross strain for 3 types of plywood (after 15 min).

which was used in the calculation of the average deceleration G. A more sophisticated calculation based on the physical properties of the wood is desirable to obtain the actual deceleration profile. No attempt was made to make such a calculation, however, because there is no information presently available for high-speed loading and large deformation of wood, and the presence of frictional effects is quite uncertain and in this series of experiments not easily evaluated.

This gross strain versus net strain equation is used to compute the maximum compression of the wood and to obtain L_M in equation (C-11).

If friction is not excessive, we can substitute E_m from equation (11) and obtain

$$G = m_2 v^2/2(m_1+m_2)g\ L_o \left\{1.14\ \sigma_n + .085[1-\exp(-11\ \sigma_n)]\right\} \quad \text{(C-13)}$$

The distance s over which the acceleration takes place is

$$s = X_3 - X_1 \quad \text{(C-14)}$$

Now

$$Fs = F(X_6 - X_4)\ s/(X_6 - X_4) \quad \text{(C-15)}$$

Using, (C-4), (C-6), and (C-8) in (C-15)

$$E_6 + E_L = E_6\ s/(X_6 - X_4) \quad \text{(C-16)}$$

From (C-1) and (C-3)

$$L_o + (X_6 - X_4) = L_F + s \quad \text{(C-17)}$$

(C-17) in (C-16) yields

$$s = (L_o - L_F)(1 + \frac{E_6}{E_L}) \quad \text{(C-18)}$$

From (C-10) and (C-11)

$$\frac{E_L}{E_M} = \frac{L_o - L_F}{L_o - L_M} \quad \text{(C-19)}$$

$$s = (L_o - L_M)(E_L + E_6)/E_M \quad \text{(C-20)}$$

$(L_o - L_M)$ may again be expressed in terms of the strain. The other quantities in (C-20) are computed or measured.

Finally the time T during which the acceleration takes place is computed from

$$T = \sqrt{\frac{2s}{gG}} \qquad \text{(C-21)}$$

where G and s are computed from (C-13) and (C-20).

APPENDIX D.—EXPRESSION OF EFFICIENCY IN TERMS OF LENGTHS AND ACCELERATIONS

We wish to express in terms of the efficiency R; (1) what length ideal gun is required to achieve v_m at the same acceleration a_o and (2) what lower acceleration a_i would produce v_m in the actual length L.

If we review our previous notations and definitions

a_o = initial acceleration in the actual gun (or maximum acceleration in the actual gun)

v_m = actually achieved muzzle velocity

L = length of actual gun

v_i = ideal velocity achievable in gun at constant acceleration a_o and length L

Now

$$v_i^2 = 2a_oL$$

and

$$R = v_m/v_i$$

we further let d be the length of ideal gun to produce v_m at constant acceleration a_o

$$\therefore v_m^2 = 2a_od$$

and

$$\frac{v_m^2}{v_i^2} = \frac{d}{L}$$

or

$$d = R^2L \tag{D-1}$$

Finally, if

a_i = ideal constant acceleration to produce v_m in a length L

then

$$v_m^2 = 2a_iL \tag{D-2}$$

or

$$a_i = R^2a_o$$

UNCLASSIFIED

Security Classification

DOCUMENT CONTROL DATA - R&D

(Security classification of title, body of abstract and indexing annotation must be entered when the overall report is classified)

1. ORIGINATING ACTIVITY *(Corporate author)* Harry Diamond Laboratories, Washington, D. C. 20438	2a. REPORT SECURITY CLASSIFICATION UNCLASSIFIED 2b. GROUP

3. REPORT TITLE

AN ARTILLERY SIMULATOR FOR FUZE EVALUATION

4. DESCRIPTIVE NOTES *(Type of report and inclusive dates)*

5. AUTHOR(S) *(Last name, first name, initial)*

Curchack, Herbert D.

6. REPORT DATE November 1966	7a. TOTAL NO. OF PAGES 64	7b. NO. OF REFS 12
8a. CONTRACT OR GRANT NO. b. PROJECT NO. DA-1P523801A301 c. AMCMS Code: 5522.11.62500 d. HDL Proj 36500	9a. ORIGINATOR'S REPORT NUMBER(S) TR-1330 9b. OTHER REPORT NO(S) *(Any other numbers that may be assigned this report)*	

10. AVAILABILITY/LIMITATION NOTICES

Qualified requesters may obtain copies of this report from DDC. DDC release to CFSTI is authorized.

11. SUPPLEMENTARY NOTES	12. SPONSORING MILITARY ACTIVITY U.S. Army Materiel Command

13. ABSTRACT

A simulator has been constructed at the Harry Diamond Laboratories for testing fuzes in an environment that provides linear and angular accelerations simultaneously as they are applied in rifled artillery weaponry. Electrical interrogation of the fuze is made during this time and subsequently while the angular velocity is maintained.

This report contains a description of the device, and a discussion of certain specific aspects of performance. It is meant to be an introduction to the technique employed, and a guide for future research and development. The performance, some results obtained, and the manner in which the simulation may be improved are described.

DD FORM 1 JAN 64 1473

UNCLASSIFIED

Security Classification

UNCLASSIFIED

Security Classification

14. KEY WORDS	LINK A ROLE	LINK A WT	LINK B ROLE	LINK B WT	LINK C ROLE	LINK C WT
Air gun, Gas gun						
Spinners						
Simulation						
Artillery simulation						
Impact						
Copper ball accelerometer						
Fuze testing						
Setback						
Spin catcher						

INSTRUCTIONS

1. ORIGINATING ACTIVITY: Enter the name and address of the contractor, subcontractor, grantee, Department of Defense activity or other organization *(corporate author)* issuing the report.

2a. REPORT SECURITY CLASSIFICATION: Enter the overall security classification of the report. Indicate whether "Restricted Data" is included. Marking is to be in accordance with appropriate security regulations.

2b. GROUP: Automatic downgrading is specified in DoD Directive 5200.10 and Armed Forces Industrial Manual. Enter the group number. Also, when applicable, show that optional markings have been used for Group 3 and Group 4 as authorized.

3. REPORT TITLE: Enter the complete report title in all capital letters. Titles in all cases should be unclassified. If a meaningful title cannot be selected without classification, show title classification in all capitals in parenthesis immediately following the title.

4. DESCRIPTIVE NOTES: If appropriate, enter the type of report, e.g., interim, progress, summary, annual, or final. Give the inclusive dates when a specific reporting period is covered.

5. AUTHOR(S): Enter the name(s) of author(s) as shown on or in the report. Enter last name, first name, middle initial. If military, show rank and branch of service. The name of the principal author is an absolute minimum requirement.

6. REPORT DATE: Enter the date of the report as day, month, year; or month, year. If more than one date appears on the report, use date of publication.

7a. TOTAL NUMBER OF PAGES: The total page count should follow normal pagination procedures, i.e., enter the number of pages containing information.

7b. NUMBER OF REFERENCES: Enter the total number of references cited in the report.

8a. CONTRACT OR GRANT NUMBER: If appropriate, enter the applicable number of the contract or grant under which the report was written.

8b, 8c, & 8d. PROJECT NUMBER: Enter the appropriate military department identification, such as project number, subproject number, system numbers, task number, etc.

9a. ORIGINATOR'S REPORT NUMBER(S): Enter the official report number by which the document will be identified and controlled by the originating activity. This number must be unique to this report.

9b. OTHER REPORT NUMBER(S): If the report has been assigned any other report numbers *(either by the originator or by the sponsor)*, also enter this number(s).

10. AVAILABILITY/LIMITATION NOTICES: Enter any limitations on further dissemination of the report, other than those imposed by security classification, using standard statements such as:

(1) "Qualified requesters may obtain copies of this report from DDC."

(2) "Foreign announcement and dissemination of this report by DDC is not authorized."

(3) "U. S. Government agencies may obtain copies of this report directly from DDC. Other qualified DDC users shall request through _____ _____."

(4) "U. S. military agencies may obtain copies of this report directly from DDC. Other qualified users shall request through _____ _____."

(5) "All distribution of this report is controlled. Qualified DDC users shall request through _____."

If the report has been furnished to the Office of Technical Services, Department of Commerce, for sale to the public, indicate this fact and enter the price, if known.

11. SUPPLEMENTARY NOTES: Use for additional explanatory notes.

12. SPONSORING MILITARY ACTIVITY: Enter the name of the departmental project office or laboratory sponsoring *(paying for)* the research and development. Include address.

13. ABSTRACT: Enter an abstract giving a brief and factual summary of the document indicative of the report, even though it may also appear elsewhere in the body of the technical report. If additional space is required, a continuation sheet shall be attached.

It is highly desirable that the abstract of classified reports be unclassified. Each paragraph of the abstract shall end with an indication of the military security classification of the information in the paragraph, represented as *(TS)*, *(S)*, *(C)*, or *(U)*.

There is no limitation on the length of the abstract. However, the suggested length is from 150 to 225 words.

14. KEY WORDS: Key words are technically meaningful terms or short phrases that characterize a report and may be used as index entries for cataloging the report. Key words must be selected so that no security classification is required. Identifiers, such as equipment model designation, trade name, military project code name, geographic location, may be used as key words but will be followed by an indication of technical context. The assignment of links, rules, and weights is optional.